Measurement of charged-particle distributions sensitive to the underlying event in $\sqrt{s} = 13\,\text{TeV}$ proton-proton collisions with the ATLAS detector at the LHC

The ATLAS collaboration

E-mail: atlas.publications@cern.ch

ABSTRACT: We present charged-particle distributions sensitive to the underlying event, measured by the ATLAS detector in proton-proton collisions at a centre-of-mass energy of 13 TeV, in low-luminosity Large Hadron Collider fills corresponding to an integrated luminosity of $1.6\,\text{nb}^{-1}$. The distributions were constructed using charged particles with absolute pseudorapidity less than 2.5 and with transverse momentum greater than 500 MeV, in events with at least one such charged particle with transverse momentum above 1 GeV. These distributions characterise the angular distribution of energy and particle flows with respect to the charged particle with highest transverse momentum, as a function of both that momentum and of charged-particle multiplicity. The results have been corrected for detector effects and are compared to the predictions of various Monte Carlo event generators, experimentally establishing the level of underlying-event activity at LHC Run 2 energies and providing inputs for the development of event generator modelling. The current models in use for UE modelling typically describe this data to 5% accuracy, compared with data uncertainties of less than 1%.

doi:10.1007/JHEP03(2017)157

Contents

1 Introduction

To perform precise Standard Model measurements or to search for new physics phenomena at hadron colliders, it is important to have a good understanding not only of the primary short-distance hard scattering process, but also of the accompanying interactions of the rest of the proton-proton collision — collectively termed the underlying event (UE). As the UE is an intrinsic part of the same proton-proton collision as any "signal" partonic interaction, accurate description of its properties by Monte Carlo (MC) event generators is important for the LHC physics programme.

In modelling terms, the UE can receive contributions from initial- and final-state radiation (ISR, FSR), from the QCD evolution of colour connections between the hard scattering and the beam-proton remnants, and from additional hard scatters in the same p-p collision, termed multiple partonic interactions (MPI). As it is significantly influenced by physics not currently calculable from first principles, the measurement of the UE's properties is crucial not only for better understanding of the mechanisms involved but also to provide input for empirical tuning of the free parameters of phenomenological UE models in MC event generators.

It is impossible to uniquely separate the UE from the hard scattering process on an event-by-event basis, but observables can be defined which are particularly sensitive to the properties of the UE. Measurements of such observables have been performed in pp collisions between $\sqrt{s} = 900\,\text{GeV}$ and $7\,\text{TeV}$ in ATLAS [1–5], ALICE [6] and CMS [7–9]. UE observables were also previously measured in $p\bar{p}$ collisions in dijet and Drell-Yan events at CDF, with centre-of-mass energies of $\sqrt{s} = 1.8\,\text{TeV}$ [10, 11] and $1.96\,\text{TeV}$ [12].

In this paper we report the measurement of UE observables with the ATLAS detector [13] at the LHC, using charged particles in $1.6\,\text{nb}^{-1}$ of proton-proton collisions at a centre-of-mass energy of $13\,\text{TeV}$.

2   Underlying-event observables

The UE observables in this study are constructed from "primary" charged particles in the pseudorapidity range $|\eta| < 2.5$,[1] whose transverse momentum (p_T) is required to be greater than $500\,\text{MeV}$. Primary charged particles are defined as those with a mean lifetime $\tau > 300\,\text{ps}$, which are either directly produced in pp interactions or from subsequent decays of particles with a lifetime $\tau < 30\,\text{ps}$. This measurement follows the fiducial particle definition used in the ATLAS $13\,\text{TeV}$ minimum-bias measurement [14] excluding particle species with τ in the range $30\,\text{ps}$ to $300\,\text{ps}$ and their decay products. The charged particles falling in this range are strange baryons with a very low reconstruction probability, whose decays are inconsistently modelled in MC generators. Their exclusion from the fiducial acceptance definition hence avoids the need to apply large and poorly defined corrections to particle level for these species, making the measurement more accurate.

This measurement uses the established form of UE observables [1–7, 9, 10, 12], in which the azimuthal plane of the event is segmented into several distinct regions with differing sensitivities to the UE. As illustrated in figure 1, the azimuthal angular difference with respect to the leading (highest-p_T) charged particle, $|\Delta\phi| = |\phi - \phi_\text{lead}|$, is used to define the regions:

- $|\Delta\phi| < 60°$, the "towards region";

- $60° < |\Delta\phi| < 120°$, the "transverse region"; and

- $|\Delta\phi| > 120°$, the "away region".

As the scale of the hard scattering increases, the leading charged particle acts as a convenient indicator of the main flow of hard-process energy. The towards and away regions are dominated by particle production from the hard process and are hence relatively insensitive to the softer UE. In contrast, the transverse region is more sensitive to the UE, and observables defined inside it are the primary focus of UE measurements.

---

[1]ATLAS uses a right-handed coordinate system with its origin at the nominal interaction point (IP) in the centre of the detector and the z-axis along the beam pipe. The x-axis points from the IP to the centre of the LHC ring, and the y-axis points upward. Cylindrical coordinates (r, ϕ) are used in the transverse plane, ϕ being the azimuthal angle around the beam pipe. The pseudorapidity is defined in terms of the polar angle θ as $\eta = -\ln\tan(\theta/2)$.
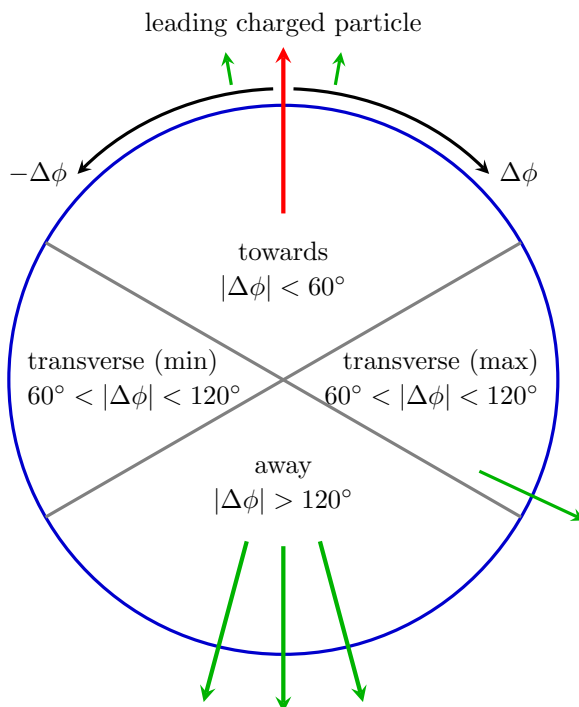
Figure 1. Definition of regions in the azimuthal angle with respect to the leading (highest-p_T) charged particle, with arrows representing particles associated with the hard scattering process and the leading charged particle highlighted in red. Conceptually, the presence of a hard-scatter particle on the right-hand side of the transverse region, increasing its $\sum p_T$, typically leads to that side being identified as the "trans-max" and hence the left-hand side as the "trans-min", with maximum sensitivity to the UE.

A further refinement is to distinguish on a per-event basis between the more and the less active sides of the transverse region [15, 16], defined in terms of their relative scalar sums of primary charged-particle p_T and termed "trans-max" and "trans-min" respectively. The trans-min region is relatively insensitive to wide-angle emissions from the hard process, and the difference between trans-max and trans-min observables (termed the "trans-diff") hence represents the effects of hard-process contamination. In this analysis, an event must have a non-zero primary charged-particle multiplicity in the trans-min region in order to be included in either the trans-min, -max, or -diff observables.

The variables measured in this analysis, constructed using charged particles with $p_T >$ 0.5 GeV and $|\eta| < 2.5$, with a higher-p_T requirement of $p_T^{\text{lead}} > 1$ GeV placed on the leading charged particle, are described in table 1. These variables are divided into two groups: first the "binned" per-event or per-particle quantities used to define the horizontal axes in the unfolded observables of section 8; and secondly the "averaged" mean values of distributions of per-event quantities to be studied as functions of the binned variables — a construction known as a "profile". The second-group variables are defined for each bin and (except for $\langle \text{mean } p_T \rangle$, in which the η–ϕ area factors cancel) are scaled by the corresponding $\delta\eta\delta\phi$ areas to give densities comparable between all such measurements,

Symbol	Description
BINNED VARIABLES	
p_T^{lead}	Transverse momentum of the leading charged particle
$N_{\text{ch}}(\text{transverse})$	Number of charged particles in the transverse region
$|\Delta\phi|$	Absolute difference in particle azimuthal angle from the leading charged particle
AVERAGED VARIABLES	
$\langle N_{\text{ch}}/\delta\eta\delta\phi \rangle$	Mean number of charged particles per unit η–ϕ (in radians)
$\langle \sum p_T/\delta\eta\delta\phi \rangle$	Mean scalar p_T sum of charged particles per unit η–ϕ (in radians)
$\langle \text{mean } p_T \rangle$	Mean per-event average p_T of charged particles (≥ 1 charged particle required)

Table 1. Definitions of the measured observables in terms of primary charged particles. The upper group of observables are used to define the x-axes of the plots to be shown in section 8, and the lower group are the mean values of distributions constructed in each x-bin and plotted on the y-axes. The $\delta\eta\delta\phi$ scale factors convert the raw measurements of regional N_{ch} and $\sum p_T$ into densities per unit η–ϕ and their values change depending on the region/bin-sizes being considered, so that the density variables are everywhere directly comparable.

including between various experiments and collider energies. The area factor $\delta\phi$ is $2\pi/3$ for the toward, transverse & away regions, whereas it is $\pi/3$ for the single-sided trans-min & trans-max regions, and $2\pi/n_{\text{bins}}$ for each of the n_{bins} equally sized bins in distributions plotted against $|\Delta\phi|$. Due to the $|\eta| < 2.5$ fiducial acceptance and the η-independence of the region definitions, $\delta\eta = 5$ in all cases. The profile observables are implemented as profile histograms, presenting the mean values of the "averaged" variables as measured in each bin of another observable. These hence measure the degree of correlation between two event features, either between the UE and hard scattering, or between different UE aspects. The mean charged-particle momentum $\langle p_T \rangle$ is constructed on an event-by-event basis and then averaged over all events to give $\langle \text{mean } p_T \rangle$.

The majority of underlying-event observables study the dependences of the averaged quantities on the transverse momentum of the leading object — here the leading charged particle. The development of this from low to high p_T corresponds to the smooth transition from "minimum bias" interactions to the hard-scattering regime focused on by most LHC analyses, and the correlation distributions characterise how soft QCD effects co-evolve with the hard process through this transition. This analysis also studies the dependence of the observables on the azimuthal angle with respect to the leading particle and each region's charged-particle multiplicity. For the observables studied as a function of relative azimuthal angle, the leading particle is excluded from the spectrum.

3 Monte Carlo modelling of the underlying event

As a physics process related to the bulk structure of protons and not calculable from first-principles perturbative QCD, the underlying event is modelled in Monte Carlo event generator programs by various phenomenological approaches. The scattering subprocess type which contributes most to UE observables is non-diffractive inelastic scattering. In event generator implementations, model-specific choices are made to regulate these pro-

cesses' QCD divergences at low scales. In this analysis the observable definitions restrict the effect of diffractive scattering, i.e. colour-singlet exchange, to play a minor role: the $\langle p_T \rangle$ profile observables have been found to be completely insensitive to diffraction, while the N_{ch} and $\sum p_T$ profiles exhibit a 2% effect at low p_T^{lead} and the whole of the N_{ch} vs. $\Delta\phi$ distribution is affected by diffraction at a 1–2% level.

This section reviews relevant features of the PYTHIA 8 [17, 18], HERWIG 7 [19] and EPOS [20, 21] MC event generator models, which are used in this study either for data correction or for comparison to the final corrected data distributions. A summary of the Monte Carlo generator configurations used is given in table 2.

Pythia 8.18 / 8.21: the PYTHIA generator family is very widely used at the LHC and elsewhere for event modelling, and PYTHIA 8 is its most recent release series. Its key features are leading-logarithmic initial- and final-state parton showers and a Lund string hadronisation model, in addition to particle decays and soft-QCD modelling. Hard-process calculations are performed either via an internal set of leading-order matrix elements, or by reading externally generated hard scattering events.

The PYTHIA 8 approach to soft-QCD modelling uses a parameterised total pp cross-section, which is split into elastic, diffractive, and non-diffractive (ND) inelastic scattering subprocesses. The first two of these again have parameterised cross-sections, and the hadronic ND inelastic cross-section is set by subtracting their contributions from the total.

The ND contribution is modelled using perturbative $2 \to 2$ QCD matrix elements, dominated by t-channel gluon exchange. As the partonic cross-section for this exceeds the hadronic ND cross-section at low p_T, the existence of MPI is implied and may be used to regularise the cross-section growth. PYTHIA 8 uses an evolved form of the Sjöstrand-van Zijl MPI model [22] in which the eikonal formalism is applied to give a model with a Poisson distribution of multiple perturbative scatterings whose mean rate depends on the scale of the hard process (interpreted as the reciprocal of the pp impact parameter), the proton form factor, and the ratio of hadronic to partonic ND cross-sections. An ansatz is used to regularise cross-section growth at low p_T, with a weak power-law evolution of the regularisation parameter with $\sqrt{s}$. The current form of the model also interleaves MPI emissions with parton shower evolution, allows several forms of matter overlap parameterisation, and interacts with a non-perturbative annealing procedure for reconfiguration of colour strings during hadronisation (the "colour reconnection" mechanism).

As MPI and hadronisation modelling are phenomenological and even the perturbative parton shower formalism has some configurational freedom, many parameter optimisations ("tunes") of PYTHIA 8 have been performed. The following are considered in this study:

- ATLAS's dedicated underlying-event tune is "A14" [23]. Its configuration is based on the NNPDF2.3 LO [24] parton density function (PDF), and was optimised for the description of several underlying event and jet radiation observ-

Generator	Version	Tune	PDF	Focus	From
PYTHIA 8	8.185	A2	MSTW2008 LO	MB	ATLAS
PYTHIA 8	8.185	A14	NNPDF2.3 LO	UE	ATLAS
PYTHIA 8	8.186	Monash	NNPDF2.3 LO	MB/UE	Authors
HERWIG 7	7.0.1	UE-MMHT	MMHT2014 LO	UE/DPS	Authors
EPOS	3.4	LHC	—	MB	Authors

Table 2. Details of the MC models used. Some tunes are focused on describing the minimum-bias (MB) distributions better, while the rest are tuned to describe underlying event (UE) or double parton scattering (DPS) distributions.

ables, including jet, Drell-Yan, and $t\bar{t}$ data, with an emphasis on high-scale events.

- An alternative tune, "Monash" [25], is used for comparison. Like A14, it was constructed using Drell-Yan and underlying-event data from ATLAS, but also data from CMS, from the SPS, and from the Tevatron in order to constrain energy scaling. It also uses the NNPDF 2.3 LO PDF, and has more of a general-purpose / low-p_{T} emphasis than A14. This tune gives an excellent description of the ATLAS 7, 8 and 13 TeV minimum-bias p_{T} spectra [14, 26, 27].

- The ATLAS minimum-bias tune "A2" [28] was used for deriving detector corrections. This is based on the MSTW2008 LO PDF [29], and was tuned using ATLAS minimum-bias data at 7 TeV for the MPI parameters, in addition to the older PYTHIA 8 tune "4C" values for fragmentation parameters. It provides a good description of minimum-bias and transverse energy flow data [30].

The PYTHIA 8 predictions shown in this paper use large MC samples from versions 8.185 and 8.186, but checks against the newer 8.2xx release series (specifically, version 8.210) found no distinguishable difference.

Herwig 7.0.1: the HERWIG family of MC generators has also been heavily used in many collider physics studies, and HERWIG 7 is the most recent major series [19, 31]. Like PYTHIA, it is a fully exclusive hadron-level generator, containing leading-logarithmic parton showers, hadronisation and decays, an MPI mechanism, and capabilities for parton-shower matching to higher-order hard processes. It uses a cluster hadronisation scheme, and angular-ordered and dipole parton showers.

The soft-QCD modelling in HERWIG 7 (and HERWIG++ before it) uses an eikonal model similar to PYTHIA's, but with some distinctions. The same treatment with Poisson-distributed simulation of many independent perturbative QCD scatters is then used, but with a simpler MPI parameterisation than in PYTHIA: the functional form of the proton electromagnetic form factor is used to parameterise the hadronic matter distribution rather than PYTHIA's very flexible parameterisation, and a continuation of eikonal scattering down to very low p_{T} values is applied in place of

PYTHIA's phenomenological regularisation of eikonal scattering below the p_T cutoff. The HERWIG soft eikonal scattering model uses distinct matter distributions for soft and hard MPI scattering, and introduces a $\sqrt{s}$-dependence of MPI parameters similar to that found in PYTHIA. The parameters of this model are highly constrained by fits to total cross-section and elastic scattering data [31, 32]. A colour-disruption mechanism is used in hadronisation, as a cluster-oriented analogy to the PYTHIA colour reconnection, to improve the quality of minimum-bias observable description.

The HERWIG 7 default tune, H7-UE-MMHT with the MMHT2014 LO PDF [33], has been used. This tune, like its HERWIG++ predecessors, is based on LHC and Tevatron underlying-event measurements, as well as double parton scattering data [34]. It provides a good description of all these observables for $\sqrt{s}$ from Tevatron 300 GeV to LHC 7 TeV.

Epos 3.4: an alternative approach is taken by EPOS, a specialist soft-QCD/cosmic-ray air-shower MC generator based on an implementation of parton-based Gribov-Regge theory [20]. This is a QCD-inspired effective-field theory describing the hard and soft scattering simultaneously. It incorporates elements of collective flow modelling from nuclear and heavy-ion physics, using hydrodynamic flow modelling in high-density regions and a string-based hadronisation model elsewhere. As a result the EPOS calculations do not make use of standard parton density functions. Using this version, equivalent to the so-called "LHC tune" of version 1.99 [21], EPOS gives a very good description of ATLAS's 13 TeV minimum-bias data, including the tails of distributions where UE physics should be involved, but as it lacks a dedicated hard scattering component it is unclear how accurate its description of UE correlations can be.

Detector-level simulation

The PYTHIA 8 A2 sample and an MC simulation of single particles distributed to populate the high-p_T region were used to derive the detector corrections for these measurements. Smaller samples produced with the EPOS generator were used to cross-check the validity of the correction procedure.

These events were processed through the ATLAS detector simulation framework [35], which is based on GEANT 4 [36]. They were then reconstructed and analysed using the same processing chain as for data. In all Monte Carlo samples the distribution of the primary vertex position was reweighted to match the distribution in data.

4   The ATLAS detector

The ATLAS detector is described in detail in ref. [13]. In this analysis, the trigger system and inner tracking detectors are of particular relevance.

The inner tracking detector is immersed in the 2 T axial magnetic field of a superconducting solenoid, and measures the trajectories of charged particles in the pseudorapidity range $|\eta| < 2.5$ with full azimuthal coverage. It consists of a silicon pixel detector (pixel), a silicon microstrip detector (SCT) and a straw-tube transition radiation tracker (TRT),

split into a barrel and two endcap components. The barrel consists of 4 pixel layers, 4 layers of SCT modules with back-to-back silicon strip sensors, and 73 layers of TRT straws; each endcap has 3 pixel layers, 9 SCT layers, and 160 TRT straw layers. The pixel, SCT and TRT have r-ϕ position resolutions of $10\,\mu\mathrm{m}$, $17\,\mu\mathrm{m}$, and $130\,\mu\mathrm{m}$ respectively, and the pixel (apart from the innermost barrel layer) and SCT have resolutions of $115\,\mu\mathrm{m}$ and $580\,\mu\mathrm{m}$ respectively in the z-direction for the barrel modules and in the r-direction for the endcaps.

The innermost pixel layer, the "insertable B-layer" (IBL), was added between LHC Runs 1 and 2, around a new narrower (radius of $25\,\mathrm{mm}$) and thinner beam pipe [37]. It is composed of 14 lightweight staves arranged in a cylindrical geometry, each made of 12 silicon planar sensors in its central region and 2×4 three-dimensional sensors at the ends. The IBL pixel dimensions are $50 \times 250\,\mu\mathrm{m}$ in the ϕ and z directions (compared with $50 \times 400\,\mu\mathrm{m}$ for other pixel layers). The smaller radius and the reduced pixel size result in improvements of both the transverse and longitudinal impact parameter resolutions. In addition, the services for the existing pixel detector were upgraded, significantly reducing the material in $|\eta| > 1.5$, in particular at the boundaries of the active tracking volume. A track from a charged particle traversing the barrel detector typically has 12 silicon measurement points (hits), of which 4 are pixel and 8 are SCT, and more than 30 TRT straw hits.

The ATLAS detector has a two-level trigger system: level 1 and the high-level trigger [38]. Events used in this analysis were required to satisfy level-1 triggers using the minimum-bias trigger scintillators (MBTS). These are mounted at each end of the detector in front of the liquid-argon endcap-calorimeter cryostats at $z = \pm 3.56\,\mathrm{m}$ and are segmented into two rings in pseudorapidity ($2.07 < |\eta| < 2.76$ and $2.76 < |\eta| < 3.86$), with 8 azimuthal sectors in the inner ring and 4 in the outer. The MBTS scintillator was replaced for Run 2 due to radiation damage incurred in Run 1. The MBTS triggers fired if at least one MBTS hit from either side of the detector was recorded above threshold.

5   Event and object selection

This measurement uses data taken in a special configuration of the LHC, with low beam currents and reduced beam focusing, producing a low mean number of interactions per bunch-crossing, $\langle\mu\rangle$, between 0.003 and 0.03. This configuration and event selection were earlier used and documented in detail in the ATLAS 13 TeV minimum-bias analysis [14], and so only a summary is given here.

Trigger: Events were selected from colliding proton bunches using a trigger which required one or more MBTS counters above threshold on either side of the detector. The efficiency of this trigger was measured to be 99% for low-multiplicity events and to rapidly rise to 100% for events with higher track multiplicities. The trigger requirement does not bias the p_T and η distributions of selected tracks in this analysis due to the $p_\mathrm{T}^\mathrm{lead} > 1\,\mathrm{GeV}$ requirement.

Primary vertex: Each event was required to contain a primary vertex reconstructed from at least two tracks with $p_\mathrm{T} > 100\,\mathrm{MeV}$ and selection requirements specific to vertexing [39]. The canonical primary vertex was identified as that with the highest $\sum p_\mathrm{T}^2$ of its

associated tracks. To reduce contamination from events with more than one interaction in a bunch crossing ("pile-up"), events containing more than one primary vertex with four or more associated tracks were removed. The contributions from non-collision backgrounds and events where two interactions are reconstructed as a single vertex were studied in data and found to be negligible.

A total of 66 million data events passed the trigger and vertex selection requirements for this analysis.

Tracks: Tracks were reconstructed starting from hits in the silicon detectors and then extrapolated to include information from the TRT. Each track required hits in both the pixel system and the SCT, including a requirement of a hit in the innermost expected pixel layer to reject secondary particles.

All tracks were reconstructed within the geometric acceptance of the inner detector, $|\eta| < 2.5$. In this analysis, all selected tracks were additionally required to have a transverse momentum above $500\,\mathrm{MeV}$, and both the transverse impact parameter and the projected longitudinal impact parameter with respect to the primary vertex were required to be less than $1.5\,\mathrm{mm}$. For high-p_T tracks, a further requirement was placed on the χ^2 probability of the track fit, to suppress mismeasured tracks. The selected events were additionally required to contain at least one track with a transverse momentum above $1\,\mathrm{GeV}$.

Backgrounds: The contributions from non-collision background events, events with more than one interaction, and fake tracks (those formed by a random combination of hits or from a combination of hits from several particles) were found to be negligible. The contribution from secondary particles was estimated as in ref. [14].

6 Correction to particle level

In order to compare the measured underlying-event distributions with model predictions in the particle-level fiducial phase space, the observables have been corrected for detector effects. These corrections include explicit accounting for inefficiencies due to the trigger selection, vertexing, and track reconstruction, by weighting the events and tracks by inverse efficiencies. A further correction has been applied to account for non-linear effects, particularly azimuthal re-orientation of the event which occurs should the leading charged particle not be reconstructed. In this situation the identification of the towards, transverse, and away regions can differ from that at particle level, leading to "wrong" track-region associations. Re-orientation mainly affects events with a low number of charged particles, and has been corrected using a dedicated method. The track-weight correction is described first, followed by the method to account for event re-orientation.

6.1 Event and track weighting

The weighting procedure for correcting measured distributions to particle level is affected by the primary vertex reconstruction efficiency, the tracking efficiency, the rate of non-primary particles, and the rate of charged strange baryons. Before defining the weights, we summarise these aspects of the vertexing and tracking performance:

Vertexing efficiency: The vertex reconstruction efficiency, ϵ_{vtx}, was determined from data by taking the ratio of the number of selected events with a reconstructed vertex to the total number of events with the requirement of a primary vertex removed. The efficiency was close to 100% except for events in which exactly one $p_{\text{T}} > 500\,\text{MeV}$ analysis track was found in the inner detector — for these the vertexing efficiency was found to be 90%. Since the leading-track $p_{\text{T}} > 1\,\text{GeV}$ requirement in the analysis is correlated with higher track multiplicities, the effect of the vertex reconstruction on the analysis is small.

Tracking efficiency: The efficiency to reconstruct primary charged particles was determined from simulation by matching MC-generator primary charged particles to tracks reconstructed from simulated inner-detector hits. For particles at the analysis transverse-momentum cutoff of $p_{\text{T}} = 500\,\text{MeV}$, the track reconstruction is $\sim 85\%$ efficient for central pseudorapidity, and decreases to 65% for $|\eta| \sim 2.5$ at the edge of the inner tracking detector; these efficiencies are higher for tracks with higher p_{T}, for example 90% and 80% respectively for $p_{\text{T}} = 10\,\text{GeV}$.

Most of the loss in tracking efficiency is due to particle interactions with the detector material and support structures, and hence a good description of the detector material is needed. The ATLAS inner tracker upgrades for LHC Run 2 necessitated a new study of the detector material uncertainties, which are detailed in ref. [14]. The track reconstruction efficiency for $|\eta| > 1.5$ is corrected using a method that compares the efficiency to extend a track reconstructed in the pixel detector into the SCT in data and simulation.

Rate of non-primary tracks: There are several sources of non-primary tracks: 1) tracks from hadronic interaction of particles with the detector material, 2) decay products from particles with strange quark content, mostly K^0 and Λ^0 decays, 3) photon conversions. The last of these is negligible for the tracks with $p_{\text{T}} > 500\,\text{MeV}$ used in this analysis. The rate of non-primary tracks was determined by comparing side-band fits of MC simulation impact parameter distributions to the data, leading to an estimated 2.3% of non-primary tracks in data for the $p_{\text{T}} > 500\,\text{MeV}$ track selection, and a smaller effect for higher-p_{T} tracks.

Fraction of charged strange baryons: Charged strange baryons and their decay products have low reconstruction efficiency, unless they have large transverse momentum. With the fiducial primary particle definition used here, the fraction of tracks due to strange baryons with $p_{\text{T}} = 10\,\text{GeV}$ is 1%, while it is much smaller than 1% at lower p_{T}. With our fiducial primary particle definition, tracks originating from charged strange baryons are classified as a background. An estimate of their contribution was made using the EPOS generator, a choice motivated both by EPOS providing the best current description of charged strange baryon rates as measured by the ALICE experiment [40], and by substantial variation of strange baryon modelling between different MC generators.

Weighting: The effect of events lost due to the trigger and vertex requirements was corrected by an event-by-event weight,

$$w_{\text{ev}}\big(n_{\text{sel}}^{\text{BL}}, \eta\big) = \frac{1}{\epsilon_{\text{trig}}\big(n_{\text{sel}}^{\text{BL}}\big)} \cdot \frac{1}{\epsilon_{\text{vtx}}\big(n_{\text{sel}}^{\text{BL}}, \eta\big)} \,, \tag{6.1}$$

where ϵ_{trig} is the trigger efficiency and $n_{\text{sel}}^{\text{BL}}$ is the multiplicity of "beam line" selected tracks, which have the same selection requirements as analysis tracks except that no vertexing requirement is applied and and hence there is no restriction on the longitudinal impact parameter. To correct for inefficiencies in the track reconstruction, the distributions of the selected analysis tracks were corrected with track-by-track weights,

$$w_{\text{trk}}(p_{\text{T}}, \eta) = \frac{1}{\epsilon_{\text{trk}}(p_{\text{T}}, \eta)} \cdot (1 - f_{\text{nonp}}(p_{\text{T}}, \eta) - f_{\text{okr}}(p_{\text{T}}, \eta) - f_{\text{sb}}(p_{\text{T}})) , \qquad (6.2)$$

where ϵ_{trk} is the tracking efficiency, and f_{nonp}, f_{okr} and f_{sb} are respectively the fractions of non-primary tracks, of out-of-kinematic-range tracks (i.e. tracks mis-reconstructed as within the fiducial p_{T} and η acceptances, but which actually originated from outside those ranges), and of weakly decaying charged strange baryons.

This track weight was used in the construction of the N_{ch}, $\sum p_{\text{T}}$, and $\Delta\phi$ distributions, and the mean p_{T} in the event, determined using the weighted average $\langle p_{\text{T}} \rangle = \sum_{i \in \text{tracks}} p_{\text{T}}^i w_{\text{trk}}^i / \sum_{i \in \text{tracks}} w_{\text{trk}}^i$.

For the distributions binned in charged multiplicity, this weight was not used to correct the binning variable, since this induces migrations subject to fluctuations not accounted for by track weighting. This correction was instead handled by the residual correction method described in the next section.

6.2 Re-orientation correction

The re-orientation correction was based on the HBOM method [41], in which the effect of the detector and reconstruction algorithms on an observable (i.e. a histogram bin value) is treated as an operator A. The observed reconstruction-level value of an observable, X^{obs}, is hence related to its true value X^{true} as $X^{\text{obs}} = AX^{\text{true}}$, but one can continue to apply A to the modified event, so that the kth additional application gives $X_k^{\text{obs}} = A^k X^{\text{obs}} = A^{k+1}X^{\text{true}}$. If the evolution of the observable's value is a smoothly varying function under such iterations, an nth-order polynomial function $P_n(k)$ can be fitted to X_k^{obs} for $k \geq 0$, and then extrapolated back to $k = -1$, i.e. X^{true}. This procedure is carried out independently for each bin of each distribution. It is distinct from the unfolding approach used in refs. [4] and [14], chosen because it is fully data-driven, i.e. does not rely on simulation performance or require reweighting of MC events to data.

In this analysis, A encodes the effects of track reconstruction, i.e. each application of A in principle smears the track kinematics and considers the possibility that some tracks would not have been reconstructed — directly inducing re-orientation should the leading track experience such a fate. These effects are described by the measured tracking resolutions and efficiencies, as functions of track η and p_{T}, but the efficiency was found to dominate and the resolution to be negligible, so A reduces to random discarding of tracks according to their reconstruction efficiency. For the profile distributions, a weight proportional to the inverse of tracking efficiency (as above) was applied in each HBOM iteration step, k, to make the effect on the observable less dramatic and more easily parameterisable. To avoid correlations between observables with different k values, each X_k^{obs} was calculated independently, using a distinct random seed and k iterations of track discarding starting

from the set of reconstructed ($k = 0$) tracks. Second-order polynomials and a maximum of $k = 4$ HBOM iterations were used as the nominal configuration, with variations being used to derive an extra systematic uncertainty, described in the following section.

7 Systematic uncertainties

Several categories of systematic uncertainties that may influence the distributions after corrections and unfolding were quantified, and their magnitudes are summarised in table 3. The sources of uncertainty and the methods used to estimate them were the following:

Trigger and vertexing: the systematic uncertainties were found to be negligible.

Track reconstruction: the uncertainties in track reconstruction efficiency principally arise from imperfect knowledge of the material in the inner detector. The new insertable B-layer and changes to pixel detector services in the $|\eta| > 1.5$ region add uncertainties not included in the inner-detector material assessments performed during Run 1: these have been evaluated by comparison of data to simulation, and by comparisons of simulations with different compositions of interacting particles. The result is an estimate of reconstruction efficiency uncertainty between 0.4% and 1.5% [14]. An additional systematic uncertainty arises from possible biases and degradation in the p_T^{lead} measurement: these effects were determined in ref. [14] and estimated to affect the tail of the p_T^{lead} distribution by 4–5%.

Non-primary particles: the systematic uncertainties were propagated by modification of track weights. The systematic uncertainty on the selected non-primary track fraction was estimated to be 24%, using variations of the fit range in the tail of the impact parameter distributions, and different MC generators and different shape assumptions for the extrapolation of the fraction from the side-bands to the signal region. The MC variation is responsible for the most significant contribution to this uncertainty. The systematic uncertainty due to the fraction of charged strange baryons was derived using the deviations of generator predictions from EPOS [14].

Unfolding: the systematic uncertainties associated with the HBOM unfolding have two distinct sources:

Non-closure: the HBOM correction procedure is in principle independent of the Monte Carlo generator modelling. However, the method shows deficiencies in some regions and distributions. The relative size of the observed non-closure (i.e. non-reproduction of a known input) derived using PYTHIA 8 A2 was therefore applied as a correction. The size of the correction is included as a systematic uncertainty, everywhere less than 2.5%. The measured transverse momentum distribution of the leading charged particle was found to be consistent with the result obtained using Bayes-inspired iterative unfolding [42] within the estimated bias.

Parameterisation: the statistical uncertainty of the HBOM method was derived for each bin using Monte Carlo sampling: for each HBOM(k) iteration, samples were

Observable	Range of values			
	Material	Non-primaries	Non-closure	Parameterisation
$N_{\rm ch}$ or $\sum p_{\rm T}$ vs. $\Delta\phi$	0.9%	0.6%	0–0.6%	0–0.4%
$N_{\rm ch}$ or $\sum p_{\rm T}$ vs. $p_{\rm T}^{\rm lead}$	0.5–1.0%	0.3–0.6%	0–2.5%	0–0.4%
$\langle$mean $p_{\rm T}\rangle$ vs. $N_{\rm ch}$	0–0.5%	0–0.5%	— 0.5% (combined) —	
$\langle$mean $p_{\rm T}\rangle$ vs. $p_{\rm T}^{\rm lead}$	0–0.4%	0–0.3%	— 0.5% (combined) —	

Table 3. Summary of systematic uncertainties for each class of UE observable, broken down by origin.

drawn from a Gaussian distribution corresponding to the point uncertainty, and 1000 independent replica HBOM fits were performed. The resulting uncertainty contribution is derived from the replicas' central 68% confidence interval. An additional systematic uncertainty, estimating the stability of the fit method, was derived by using different numbers of HBOM iterations k and polynomial degrees n.

For the results presented in the following section, these independent sources of systematic uncertainty have been combined in quadrature to form single representative systematic uncertainty estimates.

8 Results

The unfolded distributions and their main features are discussed here, and in figures 2, 3, 5 and 6 are compared to model predictions from PYTHIA 8 (the A14, A2 and Monash tunes), HERWIG 7, and EPOS. These model predictions were obtained using the analysis' associated Rivet routine [43].

Leading charged-particle $p_{\rm T}$: Figure 2 shows the unit-normalised distribution of events with respect to the transverse momentum of the leading charged particle, $p_{\rm T}^{\rm lead}$. This is a steeply falling distribution, with a change of slope for $p_{\rm T}^{\rm lead} \gtrsim 5\,{\rm GeV}$: a form which is broadly modelled by all generators. The PYTHIA 8 A14 and Monash tunes, as well as EPOS, model the distribution within 15% out to peaks strongly at the lowest $p_{\rm T}^{\rm lead}$ and alternates between under- and over-shooting the data at higher scales, finally producing a softer tail than seen in data.

Angular distributions versus leading charged particle: Figure 3 shows the mean multiplicity and $\sum p_{\rm T}$ distributions as a function of azimuthal angle with respect to the leading particle for different $p_{\rm T}^{\rm lead}$ requirements. Two event selections are shown here: the $p_{\rm T}^{\rm lead} > 1\,{\rm GeV}$ cut common to all observables, and a harder $p_{\rm T}^{\rm lead} > 10\,{\rm GeV}$ requirement.

The difference between these two selections illustrates the transition from relatively isotropic minimum-bias scattering to the emergence of hard partonic scattering structure and hence a dominant axis of energy flow. This event structure with least activity perpendicular to the leading-object axis, i.e. away from $\Delta\phi = 0°$ and $180°$, is seen for both
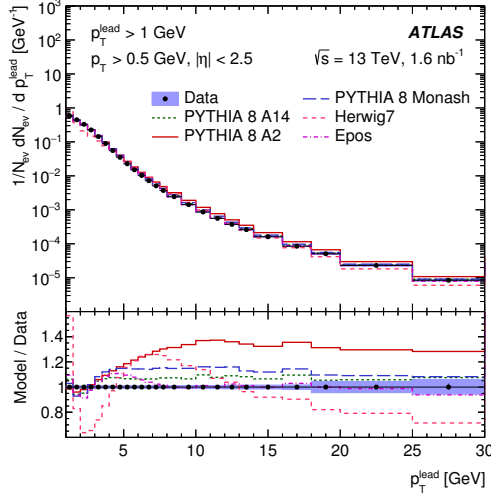
Figure 2. Unit-normalised distribution of the transverse momentum of the leading charged particle, $p_T^{lead} > 1\,\text{GeV}$, compared to various generator models. The error bars on data points represent statistical uncertainty and the blue band the total combined statistical and systematic uncertainty.
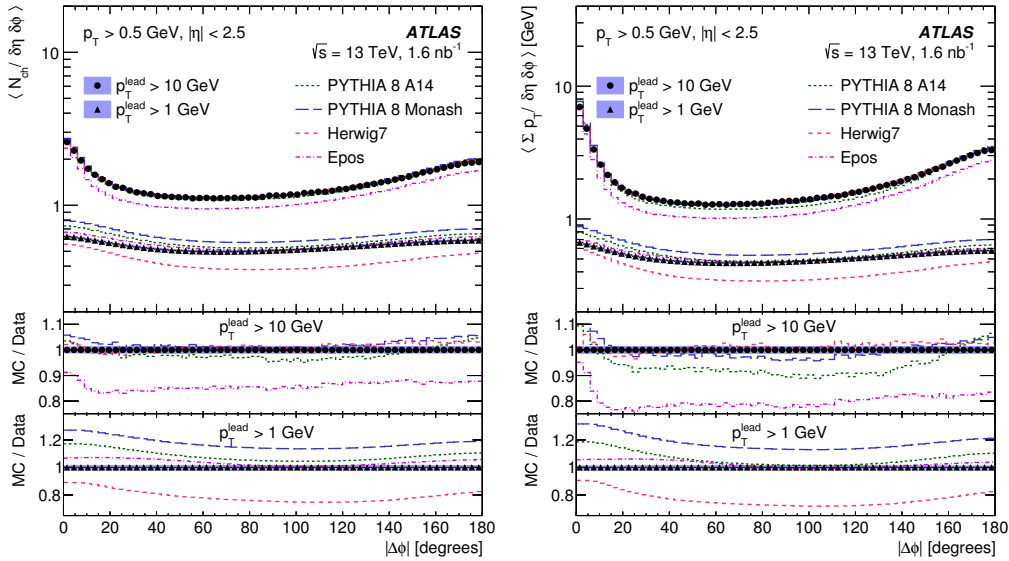

Figure 3. Distributions of mean densities of charged-particle multiplicity N_{ch} (left), and $\sum p_T$ (right) as a function of $|\Delta\phi|$ (with respect to the leading charged particle) for $p_T^{lead} > 1\,\text{GeV}$ and $p_T^{lead} > 10\,\text{GeV}$ separately, with comparisons to MC generator models. The error bars on data points represent statistical uncertainty and the blue band the total combined statistical and systematic uncertainty.
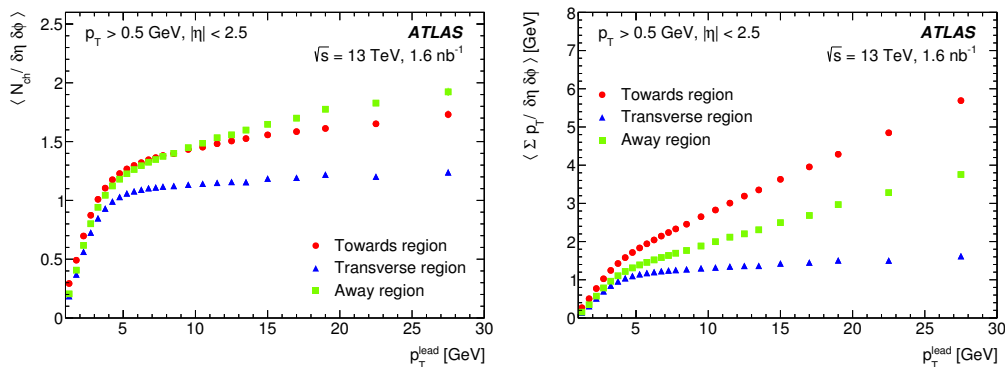
Figure 4. Mean η–ϕ densities of charged-particle multiplicities (left) and $\sum p_T$ (right) as a function of the transverse momentum of the leading charged particle in the transverse, towards, and away azimuthal regions. The error bars, which are mostly hidden by the data markers, represent combined statistical and systematic uncertainty.

selections and both observables but is much stronger for the event subset with the higher $p_T^{\text{lead}} > 10\,\text{GeV}$ requirement: this demonstrates the evolution of event shape as a hard scattering component develops.

There is no clear "best" MC model for these observables. EPOS performs best in the more inclusive $p_T^{\text{lead}} > 1\,\text{GeV}$ selection, followed by PYTHIA 8 A14; HERWIG 7 significantly undershoots while PYTHIA 8 Monash is everywhere above the data. But in the hard-scattering $p_T^{\text{lead}} > 10\,\text{GeV}$ event selection, HERWIG 7 and Monash perform best, with a slight undershoot from PYTHIA 8 A14 and a large one from EPOS. These orderings apply to both the N_{ch} and $\sum p_T$ variables, although to different extents.

N_{ch} and $\sum p_T$ densities in transverse/towards/away regions: Figure 4 shows the evolution of the mean charged-particle multiplicity and $\sum p_T$ densities with the p_T of the leading charged particle, from 1 to 30 GeV. For both observables, the towards, transverse, and away regions are shown overlaid for ease of comparison.

The primary feature is the general shape seen in all curves: starting close to zero at low p_T^{lead}, there is first a very rapid rise in activity in which the three regions are not strongly distinguished, then an abrupt transition at $p_T^{\text{lead}} \approx 5\,\text{GeV}$ above which the three regions have quite distinct behaviours. The initial rapid rise to a roughly stable value of ~1 charged particle or ~1 GeV per unit η–ϕ area is known as the "pedestal effect". In modelling terms this reflects a reduction of the pp impact parameter with increasing p_T^{lead}, and hence the transition between the minimum-bias and hard-scattering regimes.

Secondly, the shape of the transverse region is different from the other two in both observables — it almost completely plateaus after $p_T^{\text{lead}} \approx 5\,\text{GeV}$, while the towards and away regions continue to rise nearly linearly with p_T^{lead}. This characteristic feature of UE profile observables is the empirical demonstration of the azimuthal-region paradigm for UE analysis: the hard process dominates the towards and away regions, which continue to increase in activity as the hard-process scale grows, but the transverse region is relatively unaffected. This is consistent with the pedestal effect where the overlap between

colliding protons is complete and hence any further growth is due to connections to, or contaminations from, the hard process rather than more MPI scattering.

An interesting feature is that for $p_T^{\text{lead}} \gtrsim 7\,\text{GeV}$ the *away* region actually becomes the one with highest charged-particle multiplicity, despite not containing the highest-p_T charged particle. By the $\sum p_T$ density measure, however, the towards region is unambiguously the most active region for all p_T^{lead} values.

N_{ch} and $\sum p_T$ densities in trans-min/max/diff regions: Figure 5 focuses on the UE-dominated transverse region, and its per-event specialisations trans-min, -max, and -diff. Between these, the trans-min is the most sensitive to MPI effects, i.e. the pedestal, while the trans-max includes both MPI and hard-process contaminations: the trans-diff is hence the clearest measure of those contaminations. The comparisons to MC models are again made in these plots.

There is significant variation in performance between the models, with PYTHIA 8's Monash tune and HERWIG 7 giving the best description of data in the plateau region of trans-min, followed within 10% by the other PYTHIA 8 tunes. EPOS, however, slightly overestimates in the "ramp" region to the pedestal effect plateau, and on the plateau it underestimates the pedestal height by around 20%. HERWIG 7 and PYTHIA 8 A2 both mismodel the transition, with a severe undershoot for HERWIG below p_T^{lead} of $5\,\text{GeV}$, and a milder but broader undershoot from A2 which extends up to $p_T^{\text{lead}} \approx 20\,\text{GeV}$.

The predictions cluster together more tightly in the process-inclusive trans-max region, with all generators other than EPOS providing a description of the N_{ch} density data within a few percent for $p_T^{\text{lead}} \geq 10\,\text{GeV}$; EPOS continues to undershoot the data significantly. PYTHIA 8 A14 also significantly undershoots the $\sum p_T$ density data, by around 10% as compared to EPOS's 20%. Looking in trans-diff gives a clearer view of how non-MPI contributions to the UE are modelled, with mostly flat ~10% overshoots from all models other than EPOS in N_{ch} density, and a spread of performance in describing the $\sum p_T$ density evolution. In the latter the best performance comes from the PYTHIA 8 Monash and A2 tunes, with HERWIG 7 and PYTHIA 8 A14 both wrong by 5–10% but in opposite directions — EPOS's prediction is again separated from the ATLAS data by more than 20%.

There is no obvious best model for all observables, but the PYTHIA 8 Monash tune agrees well with the data in all observables other than trans-diff N_{ch} density, and HERWIG 7 has comparable performance for hard-scattering events away from the "minimum-bias region" of $p_T^{\text{lead}} < 5\,\text{GeV}$. The PYTHIA 8 A14 tune, used for much of the hard-process simulation in ATLAS, predicts activity 5% to 10% below the data, indicating that some re-tuning for $13\,\text{TeV}$ event modelling may yield performance benefits. EPOS is not able to model the level of underlying-event activity well in events with higher p_T^{lead}.

Mean transverse momentum in transverse & trans/min/max regions: The per-event mean transverse momentum of charged particles in the transverse azimuthal regions is of interest since it illustrates the balance in UE physics between the $\sum p_T$ and multiplicity observables. This balance is affected in some MC models by colour-reconnection or -disruption mechanisms, which stochastically reconfigure the colour structures in the hadronising system into energetically favourable states and typically increase the p_T per particle.
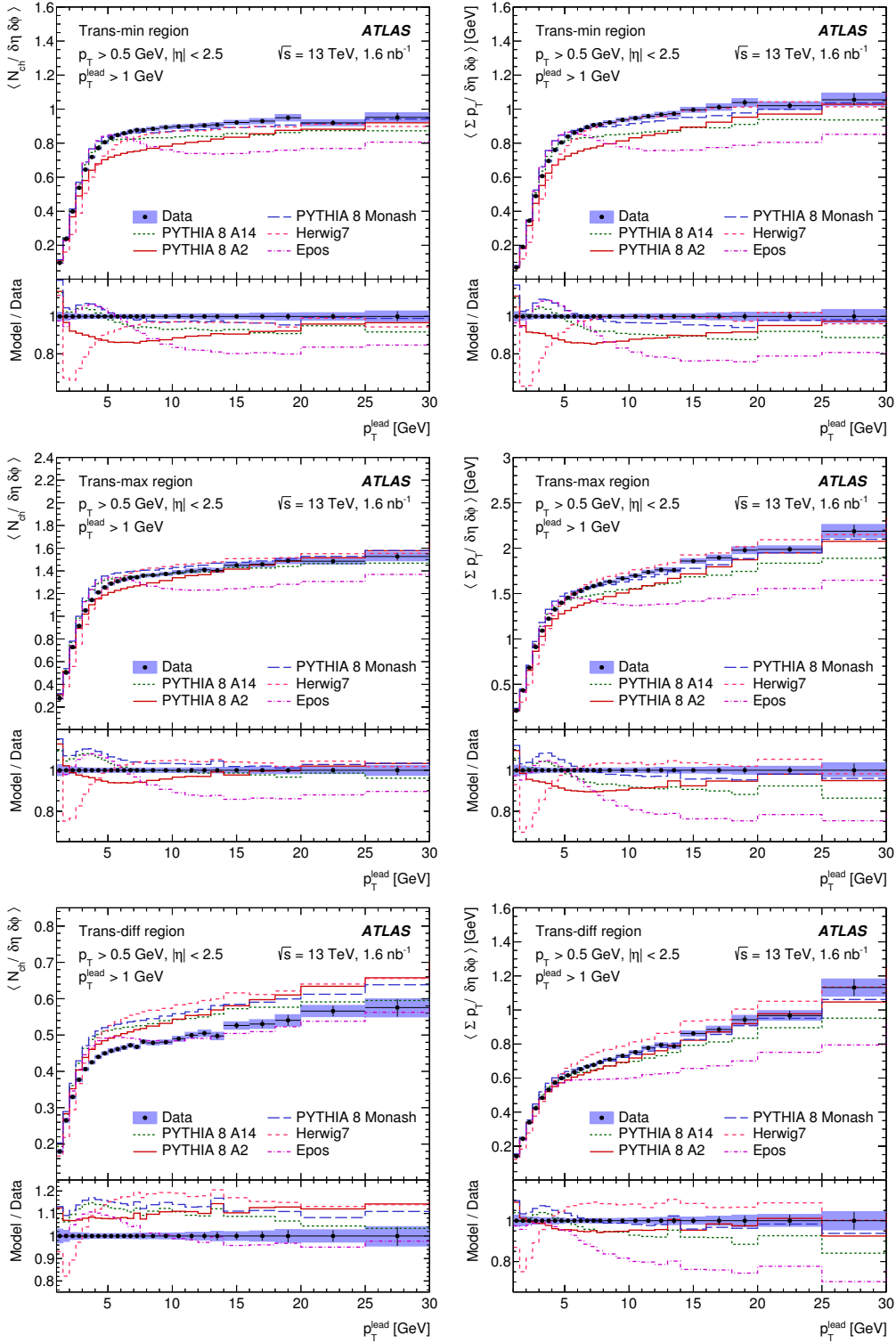
Figure 5. Mean densities of charged-particle multiplicity N_{ch} (left) and $\sum p_T$ (right) as a function of leading charged-particle p_T, in the trans-min (top), trans-max (middle) and trans-diff (bottom) azimuthal regions. The error bars on data points represent statistical uncertainty and the blue band the total combined statistical and systematic uncertainty.

Measurements of the correlations of mean p_T with other event features are an important input to constrain such *ad hoc* models. Figure 6 shows, for the transverse and trans-min/max azimuthal regions, the correlations of the average per-event mean transverse momentum, $\langle \text{mean } p_T \rangle$, with the transverse region's charged-particle multiplicity and the event's p_T^{lead}.

The correlation with transverse charged-particle multiplicity N_{ch} is a correlation between two different "soft" properties. This distribution is modelled to within 5% for all N_{ch} by most of the generators and in all transverse region variants, but in all cases an underestimation of $\langle \text{mean } p_T \rangle$ is visible until $N_{\text{ch}} \gtrsim 15$. The best modelling is from EPOS, whose maximum undershoot is $\sim$3% at low N_{ch} but which follows the data closely in all region definitions for higher transverse multiplicities. The Monash tune is the best-performing PYTHIA 8 configuration, with a performance similar to that of EPOS, while PYTHIA 8 A14 undershoots in the low-multiplicity events and PYTHIA 8 A2 overshoots at high-multiplicities — notably the regions not included in each tune's construction. HER-WIG 7 shows the largest variations, from a $\sim$7% undershoot at low N_{ch} to a 5% overshoot at $N_{\text{ch}} \approx 30$.

However, HERWIG 7 performs better than all the other generators when considering the correlation between transverse region $\langle \text{mean } p_T \rangle$ and p_T^{lead}. As seen in figure 5, the transverse $\sum p_T$ does not reach as flat a plateau as does N_{ch} with increasing p_T^{lead}, and hence the event-wise $\langle \text{mean } p_T \rangle$ increases with p_T^{lead}. HERWIG's behaviour in this observable is within 1% of the data except in the "minimum bias" $p_T^{\text{lead}} \lesssim 5 \, \text{GeV}$ phase space (where the HERWIG model is not expected to work), while all PYTHIA 8 tunes undershoot the data by between 5% and 10%, and EPOS even more so.
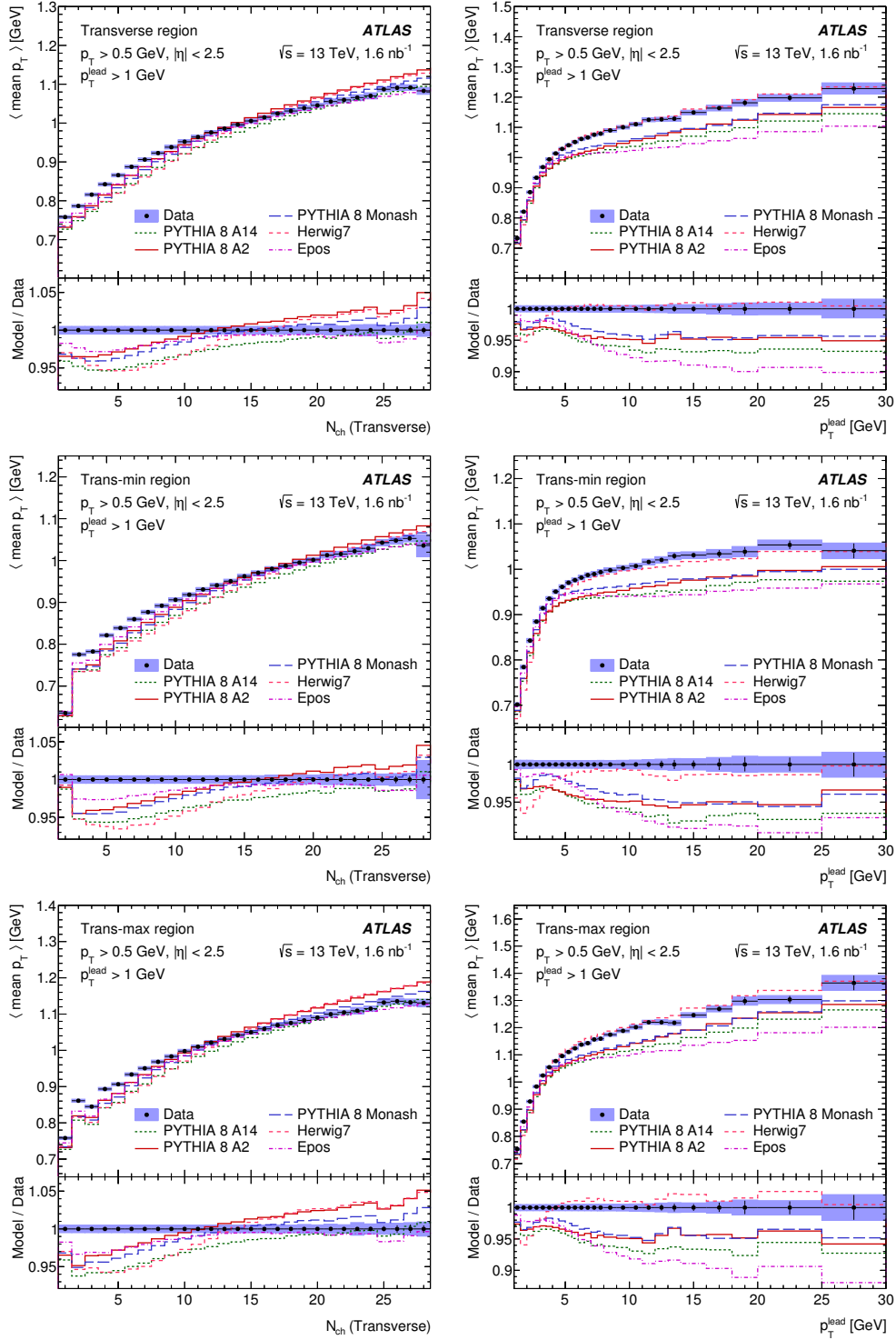
Figure 6. Mean charged-particle average transverse momentum as a function of charged-particle multiplicity in transverse region N_{ch}(Transverse) (left) and as a function of p_T^{lead} (right), for each of the transverse (top), trans-min (middle) and trans-max (bottom) azimuthal regions. The error bars on data points represent statistical uncertainty and the blue band the total combined statistical and systematic uncertainty.
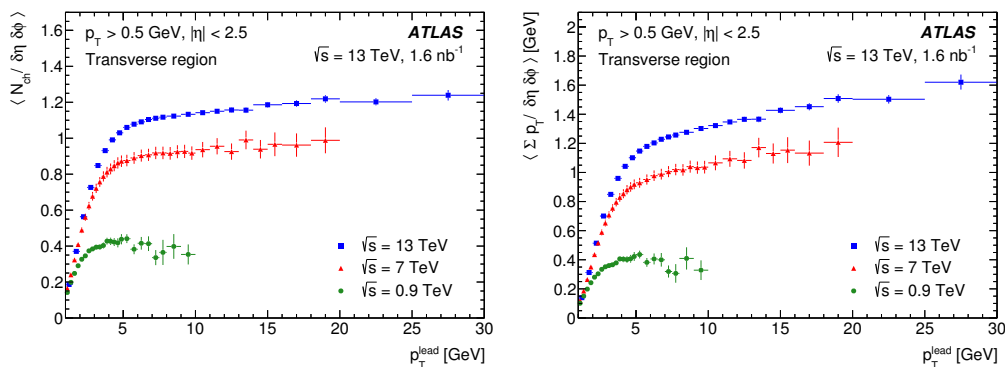
Figure 7. Mean charged-particle multiplicity (left) and $\sum p_T$ (right) densities as a function of transverse momentum of the leading charged particle measured for $\sqrt{s} = 0.9, 7\,\text{TeV}$ [1] and $13\,\text{TeV}$ centre-of-mass energies. The fiducial acceptance definitions of the $\sqrt{s} = 0.9$ and $7\,\text{TeV}$ measurements did not exclude charged strange baryons, but this effect is limited to a few percent at most.

9 Conclusions

We have presented several distributions sensitive to properties of the underlying event, measured by the ATLAS experiment at the LHC using $1.6\,\text{nb}^{-1}$ of low-luminosity $13\,\text{TeV}$ pp collision events. The measured observables are defined using charged tracks and have been corrected to the level of primary charged particles. Correction of the results for detector effects was performed via a combination of tracking and vertexing efficiency weighting and HBOM unfolding, with the latter accounting for re-orientation and similar indirect effects not accounted for by the reweighting. Systematic uncertainties are included for the effects of all data processing steps, including the unfolding.

The analysis observables follow the established strategy in which each event is azimuthally segmented into "towards", "transverse", and "away" regions with respect to the highest-p_T ("leading") charged particle, with a further per-event distinction into "min" and "max" sides within the transverse region. This construction produces a set of observables collectively sensitive to each of the components of the underlying event. The observables in this study characterise the correlations of a) each azimuthal region's mean $\sum p_T$ and mean charged-particle multiplicity densities with the transverse momentum, p_T^{lead}, of the event's leading charged particle; and b) the per-event mean charged-particle p_T with both p_T^{lead} and the transverse azimuthal region's charged-particle multiplicity. The correlations with p_T^{lead} characterise the degree of connection between the underlying event and the hardest partonic scattering in the pp collision, while correlations with the transverse regions' charged-particle multiplicities probe the particle production mechanisms between underlying-event components.

The presented measurement improves upon previous ATLAS measurements of the underlying event using leading-track alignment, both in the reach in p_T^{lead} and the precision achieved. Figure 7 shows the transverse region's mean N_{ch} and $\sum p_T$ densities in bins of p_T^{lead} as measured in leading-charged-particle UE studies at $\sqrt{s} = 0.9$ and $7\,\text{TeV}$, compared with the new $13\,\text{TeV}$ data. An increase in UE activity of approximately 20% is observed when going from $7\,\text{TeV}$ to $13\,\text{TeV}$ pp collisions.

These results are a crucial input to physics studies in LHC pp collisions throughout the 13 TeV run, since the underlying event is present in all inelastic collision processes. Comparisons against predictions from several commonly used MC generator configurations indicate that for most observables the models describe the underlying-event data to better than 5% accuracy. But this level of variation is far greater than the experimental uncertainty of the measurements, and there is evidence of systematic mismodelling. The model defects are particularly acute in the transition from generic soft inelastic interactions — so-called "minimum bias" scattering — to secondary interactions in the presence of hard partonic scattering. Some improvement to MC tunes in light of these data will hence be of benefit to physics studies in LHC Run 2. The Epos MC generator, specialised for simulation of inclusive soft QCD processes, displays particularly discrepant features as the $p_{\mathrm{T}}^{\mathrm{lead}}$ scale increases, casting doubt on its suitability for modelling LHC multiple pp interactions despite currently providing the best description of minimum-bias data.

This study hence provides important data from the new collider energy frontier for the tuning of MC generators in LHC Run 2, and further incentives for the development of a nucleon collision model capable of describing collider data in both hard and soft scatterings and at multiple centre-of-mass energies.

Acknowledgments

The crucial computing support from all WLCG partners is acknowledged gratefully, in particular from CERN, the ATLAS Tier-1 facilities at TRIUMF (Canada), NDGF (Denmark, Norway, Sweden), CC-IN2P3 (France), KIT/GridKA (Germany), INFN-CNAF (Italy), NL-T1 (Netherlands), PIC (Spain), ASGC (Taiwan), RAL (U.K.) and BNL (U.S.A.), the Tier-2 facilities worldwide and large non-WLCG resource providers. Major contributors of computing resources are listed in ref. [44].

References

[1] ATLAS collaboration, *Measurement of underlying event characteristics using charged particles in pp collisions at $\sqrt{s} = 900\,GeV$ and $7\,TeV$ with the ATLAS detector*, *Phys. Rev.* **D 83** (2011) 112001 [arXiv:1012.0791] [INSPIRE].

[2] ATLAS collaboration, *Measurements of underlying-event properties using neutral and charged particles in pp collisions at $900\,GeV$ and $7\,TeV$ with the ATLAS detector at the LHC*, *Eur. Phys. J.* **C 71** (2011) 1636 [arXiv:1103.1816] [INSPIRE].

[3] ATLAS collaboration, *Underlying event characteristics and their dependence on jet size of charged-particle jet events in pp collisions at $\sqrt{s} = 7\,TeV$ with the ATLAS detector*, *Phys. Rev.* **D 86** (2012) 072004 [arXiv:1208.0563] [INSPIRE].

[4] ATLAS collaboration, *Measurement of the underlying event in jet events from $7\,TeV$ proton-proton collisions with the ATLAS detector*, *Eur. Phys. J.* **C 74** (2014) 2965 [arXiv:1406.0392] [INSPIRE].

[5] ATLAS collaboration, *Measurement of distributions sensitive to the underlying event in inclusive Z-boson production in pp collisions at $\sqrt{s} = 7\,TeV$ with the ATLAS detector*, *Eur. Phys. J.* **C 74** (2014) 3195 [arXiv:1409.3433] [INSPIRE].

[6] ALICE collaboration, *Underlying event measurements in pp collisions at $\sqrt{s} = 0.9$ and $7\,TeV$ with the ALICE experiment at the LHC*, *JHEP* **07** (2012) 116 [arXiv:1112.2082] [INSPIRE].

[7] CMS collaboration, *First measurement of the underlying event activity at the LHC with $\sqrt{s} = 0.9\,TeV$*, *Eur. Phys. J.* **C 70** (2010) 555 [arXiv:1006.2083] [INSPIRE].

[8] CMS collaboration, *Measurement of the underlying event activity using charged-particle jets in proton-proton collisions at $\sqrt{s} = 2.76\,TeV$*, *JHEP* **09** (2015) 137 [arXiv:1507.07229] [INSPIRE].

[9] CMS collaboration, *Measurement of the underlying event in the Drell-Yan process in proton-proton collisions at $\sqrt{s} = 7\,TeV$*, *Eur. Phys. J.* **C 72** (2012) 2080 [arXiv:1204.1411] [INSPIRE].

[10] CDF collaboration, T. Affolder et al., *Charged jet evolution and the underlying event in $p\bar{p}$ collisions at $1.8\,TeV$*, *Phys. Rev.* **D 65** (2002) 092002 [INSPIRE].

[11] CDF collaboration, D. Acosta et al., *The underlying event in hard interactions at the Tevatron $\bar{p}p$ collider*, *Phys. Rev.* **D 70** (2004) 072002 [hep-ex/0404004] [INSPIRE].

[12] CDF collaboration, T. Aaltonen et al., *Studying the underlying event in Drell-Yan and high transverse momentum jet production at the Tevatron*, *Phys. Rev.* **D 82** (2010) 034001 [arXiv:1003.3146] [INSPIRE].

[13] ATLAS collaboration, *The ATLAS experiment at the CERN Large Hadron Collider*, 2008 *JINST* **3** S08003 [INSPIRE].

[14] ATLAS collaboration, *Charged-particle distributions in* $\sqrt{s} = 13\,TeV$ *pp interactions measured with the ATLAS detector at the LHC*, *Phys. Lett.* **B 758** (2016) 67 [arXiv:1602.01633] [INSPIRE].

[15] G. Marchesini and B.R. Webber, *Associated transverse energy in hadronic jet production*, *Phys. Rev.* **D 38** (1988) 3419 [INSPIRE].

[16] J. Pumplin, *Hard underlying event correction to inclusive jet cross-sections*, *Phys. Rev.* **D 57** (1998) 5787 [hep-ph/9708464] [INSPIRE].

[17] T. Sjöstrand, S. Mrenna and P.Z. Skands, *A brief introduction to PYTHIA 8.1*, *Comput. Phys. Commun.* **178** (2008) 852 [arXiv:0710.3820] [INSPIRE].

[18] T. Sjöstrand, S. Mrenna and P.Z. Skands, *PYTHIA 6.4 physics and manual*, *JHEP* **05** (2006) 026 [hep-ph/0603175] [INSPIRE].

[19] J. Bellm et al., *HERWIG 7.0/HERWIG++ 3.0 release note*, *Eur. Phys. J.* **C 76** (2016) 196 [arXiv:1512.01178] [INSPIRE].

[20] T. Pierog and K. Werner, *EPOS model and ultra high energy cosmic rays*, [*Nucl. Phys. Proc. Suppl.* **B 196** (2009) 102] [arXiv:0905.1198] [INSPIRE].

[21] T. Pierog, I. Karpenko, J.M. Katzy, E. Yatsenko and K. Werner, *EPOS LHC: test of collective hadronization with data measured at the CERN Large Hadron Collider*, *Phys. Rev.* **C 92** (2015) 034906 [arXiv:1306.0121] [INSPIRE].

[22] T. Sjöstrand and M. van Zijl, *A multiple interaction model for the event structure in hadron collisions*, *Phys. Rev.* **D 36** (1987) 2019 [INSPIRE].

[23] ATLAS collaboration, *ATLAS Run 1 PYTHIA8 tunes*, ATL-PHYS-PUB-2014-021, CERN, Geneva Switzerland, (2014).

[24] R.D. Ball et al., *Parton distributions with LHC data*, *Nucl. Phys.* **B 867** (2013) 244 [arXiv:1207.1303] [INSPIRE].

[25] P. Skands, S. Carrazza and J. Rojo, *Tuning PYTHIA 8.1: the Monash 2013 tune*, *Eur. Phys. J.* **C 74** (2014) 3024 [arXiv:1404.5630] [INSPIRE].

[26] ATLAS collaboration, *Charged-particle multiplicities in pp interactions measured with the ATLAS detector at the LHC*, *New J. Phys.* **13** (2011) 053033 [arXiv:1012.5104] [INSPIRE].

[27] ATLAS collaboration, *Charged-particle distributions in pp interactions at* $\sqrt{s} = 8\,TeV$ *measured with the ATLAS detector*, *Eur. Phys. J.* **C 76** (2016) 403 [arXiv:1603.02439] [INSPIRE].

[28] ATLAS collaboration, *Further ATLAS tunes of PYTHIA6 and PYTHIA8*, ATL-PHYS-PUB-2011-014, CERN, Geneva Switzerland, (2011).

[29] A.D. Martin, W.J. Stirling, R.S. Thorne and G. Watt, *Parton distributions for the LHC*, *Eur. Phys. J.* **C 63** (2009) 189 [arXiv:0901.0002] [INSPIRE].

[30] ATLAS collaboration, *Measurements of the pseudorapidity dependence of the total transverse energy in proton-proton collisions at $\sqrt{s} = 7$ TeV with ATLAS*, *JHEP* **11** (2012) 033 [arXiv:1208.6256] [INSPIRE].

[31] M. Bahr et al., *HERWIG++ physics and manual*, *Eur. Phys. J.* **C 58** (2008) 639 [arXiv:0803.0883] [INSPIRE].

[32] M. Bahr, J.M. Butterworth and M.H. Seymour, *The underlying event and the total cross section from Tevatron to the LHC*, *JHEP* **01** (2009) 065 [arXiv:0806.2949] [INSPIRE].

[33] L.A. Harland-Lang, A.D. Martin, P. Motylinski and R.S. Thorne, *Parton distributions in the LHC era: MMHT 2014 PDFs*, *Eur. Phys. J.* **C 75** (2015) 204 [arXiv:1412.3989] [INSPIRE].

[34] M.H. Seymour and A. Siodmok, *Constraining MPI models using σ_{eff} and recent Tevatron and LHC underlying event data*, *JHEP* **10** (2013) 113 [arXiv:1307.5015] [INSPIRE].

[35] ATLAS collaboration, *The ATLAS simulation infrastructure*, *Eur. Phys. J.* **C 70** (2010) 823 [arXiv:1005.4568] [INSPIRE].

[36] GEANT4 collaboration, S. Agostinelli et al., *GEANT4: a simulation toolkit*, *Nucl. Instrum. Meth.* **A 506** (2003) 250 [INSPIRE].

[37] ATLAS collaboration, *ATLAS insertable B-layer technical design report*, CERN-LHCC-2010-013, CERN, Geneva Switzerland, (2010) [CERN-LHCC-2010-013] [ATLAS-TDR-19].

[38] ATLAS collaboration, 2015 *start-up trigger menu and initial performance assessment of the ATLAS trigger using Run-2 data*, ATL-DAQ-PUB-2016-001, CERN, Geneva Switzerland, (2016).

[39] G. Piacquadio, K. Prokofiev and A. Wildauer, *Primary vertex reconstruction in the ATLAS experiment at LHC*, *J. Phys. Conf. Ser.* **119** (2008) 032033 [INSPIRE].

[40] ALICE collaboration, *Strange particle production in proton-proton collisions at $\sqrt{s} = 0.9$ TeV with ALICE at the LHC*, *Eur. Phys. J.* **C 71** (2011) 1594 [arXiv:1012.3257] [INSPIRE].

[41] J.W. Monk and C. Oropeza-Barrera, *The HBOM method for unfolding detector effects*, *Nucl. Instrum. Meth.* **A 701** (2013) 17 [arXiv:1111.4896] [INSPIRE].

[42] G. D'Agostini, *A multidimensional unfolding method based on Bayes' theorem*, *Nucl. Instrum. Meth.* **A 362** (1995) 487 [INSPIRE].

[43] A. Buckley et al., *Rivet user manual*, *Comput. Phys. Commun.* **184** (2013) 2803 [arXiv:1003.0694] [INSPIRE].

[44] ATLAS collaboration, *ATLAS computing acknowledgements* 2016–2017, ATL-GEN-PUB-2016-002, CERN, Geneva Switzerland, (2016).

The ATLAS collaboration

M. Aaboud[137d], G. Aad[88], B. Abbott[115], J. Abdallah[8], O. Abdinov[12], B. Abeloos[119],
S.H. Abidi[161], O.S. AbouZeid[139], N.L. Abraham[151], H. Abramowicz[155], H. Abreu[154], R. Abreu[118],
Y. Abulaiti[148a,148b], B.S. Acharya[167a,167b,a], S. Adachi[157], L. Adamczyk[41a], D.L. Adams[27],
J. Adelman[110], M. Adersberger[102], T. Adye[133], A.A. Affolder[139], T. Agatonovic-Jovin[14],
C. Agheorghiesei[28b], J.A. Aguilar-Saavedra[128a,128f], S.P. Ahlen[24], F. Ahmadov[68,b],
G. Aielli[135a,135b], S. Akatsuka[71], H. Akerstedt[148a,148b], T.P.A. Åkesson[84], A.V. Akimov[98],
G.L. Alberghi[22a,22b], J. Albert[172], M.J. Alconada Verzini[74], M. Aleksa[32], I.N. Aleksandrov[68],
C. Alexa[28b], G. Alexander[155], T. Alexopoulos[10], M. Alhroob[115], B. Ali[130], M. Aliev[76a,76b],
G. Alimonti[94a], J. Alison[33], S.P. Alkire[38], B.M.M. Allbrooke[151], B.W. Allen[118], P.P. Allport[19],
A. Aloisio[106a,106b], A. Alonso[39], F. Alonso[74], C. Alpigiani[140], A.A. Alshehri[56], M. Alstaty[88],
B. Alvarez Gonzalez[32], D. Álvarez Piqueras[170], M.G. Alviggi[106a,106b], B.T. Amadio[16],
Y. Amaral Coutinho[26a], C. Amelung[25], D. Amidei[92], S.P. Amor Dos Santos[128a,128c],
A. Amorim[128a,128b], S. Amoroso[32], G. Amundsen[25], C. Anastopoulos[141], L.S. Ancu[52],
N. Andari[19], T. Andeen[11], C.F. Anders[60b], J.K. Anders[77], K.J. Anderson[33], A. Andreazza[94a,94b],
V. Andrei[60a], S. Angelidakis[9], I. Angelozzi[109], A. Angerami[38], F. Anghinolfi[32],
A.V. Anisenkov[111,c], N. Anjos[13], A. Annovi[126a,126b], C. Antel[60a], M. Antonelli[50], A. Antonov[100,*],
D.J. Antrim[166], F. Anulli[134a], M. Aoki[69], L. Aperio Bella[32], G. Arabidze[93], Y. Arai[69],
J.P. Araque[128a], V. Araujo Ferraz[26a], A.T.H. Arce[48], R.E. Ardell[80], F.A. Arduh[74], J-F. Arguin[97],
S. Argyropoulos[66], M. Arik[20a], A.J. Armbruster[145], L.J. Armitage[79], O. Arnaez[32], H. Arnold[51],
M. Arratia[30], O. Arslan[23], A. Artamonov[99], G. Artoni[122], S. Artz[86], S. Asai[157], N. Asbah[45],
A. Ashkenazi[155], L. Asquith[151], K. Assamagan[27], R. Astalos[146a], M. Atkinson[169], N.B. Atlay[143],
K. Augsten[130], G. Avolio[32], B. Axen[16], M.K. Ayoub[119], G. Azuelos[97,d], A.E. Baas[60a],
M.J. Baca[19], H. Bachacou[138], K. Bachas[76a,76b], M. Backes[122], M. Backhaus[32],
P. Bagiacchi[134a,134b], P. Bagnaia[134a,134b], J.T. Baines[133], M. Bajic[39], O.K. Baker[179],
E.M. Baldin[111,c], P. Balek[175], T. Balestri[150], F. Balli[138], W.K. Balunas[124], E. Banas[42],
Sw. Banerjee[176,e], A.A.E. Bannoura[178], L. Barak[32], E.L. Barberio[91], D. Barberis[53a,53b],
M. Barbero[88], T. Barillari[103], M-S Barisits[32], T. Barklow[145], N. Barlow[30], S.L. Barnes[36c],
B.M. Barnett[133], R.M. Barnett[16], Z. Barnovska-Blenessy[36a], A. Baroncelli[136a], G. Barone[25],
A.J. Barr[122], L. Barranco Navarro[170], F. Barreiro[85], J. Barreiro Guimarães da Costa[35a],
R. Bartoldus[145], A.E. Barton[75], P. Bartos[146a], A. Basalaev[125], A. Bassalat[119,f], R.L. Bates[56],
S.J. Batista[161], J.R. Batley[30], M. Battaglia[139], M. Bauce[134a,134b], F. Bauer[138], H.S. Bawa[145,g],
J.B. Beacham[113], M.D. Beattie[75], T. Beau[83], P.H. Beauchemin[165], P. Bechtle[23], H.P. Beck[18,h],
K. Becker[122], M. Becker[86], M. Beckingham[173], C. Becot[112], A.J. Beddall[20e], A. Beddall[20b],
V.A. Bednyakov[68], M. Bedognetti[109], C.P. Bee[150], T.A. Beermann[32], M. Begalli[26a], M. Begel[27],
J.K. Behr[45], A.S. Bell[81], G. Bella[155], L. Bellagamba[22a], A. Bellerive[31], M. Bellomo[89],
K. Belotskiy[100], O. Beltramello[32], N.L. Belyaev[100], O. Benary[155,*], D. Benchekroun[137a],
M. Bender[102], K. Bendtz[148a,148b], N. Benekos[10], Y. Benhammou[155], E. Benhar Noccioli[179],
J. Benitez[66], D.P. Benjamin[48], M. Benoit[52], J.R. Bensinger[25], S. Bentvelsen[109], L. Beresford[122],
M. Beretta[50], D. Berge[109], E. Bergeaas Kuutmann[168], N. Berger[5], J. Beringer[16], S. Berlendis[58],
N.R. Bernard[89], G. Bernardi[83], C. Bernius[112], F.U. Bernlochner[23], T. Berry[80], P. Berta[131],
C. Bertella[86], G. Bertoli[148a,148b], F. Bertolucci[126a,126b], I.A. Bertram[75], C. Bertsche[45],
D. Bertsche[115], G.J. Besjes[39], O. Bessidskaia Bylund[148a,148b], M. Bessner[45], N. Besson[138],
C. Betancourt[51], A. Bethani[87], S. Bethke[103], A.J. Bevan[79], R.M. Bianchi[127], M. Bianco[32],
O. Biebel[102], D. Biedermann[17], R. Bielski[87], N.V. Biesuz[126a,126b], M. Biglietti[136a],
J. Bilbao De Mendizabal[52], T.R.V. Billoud[97], H. Bilokon[50], M. Bindi[57], A. Bingul[20b],
C. Bini[134a,134b], S. Biondi[22a,22b], T. Bisanz[57], C. Bittrich[47], D.M. Bjergaard[48], C.W. Black[152],

J.E. Black[145], K.M. Black[24], D. Blackburn[140], R.E. Blair[6], T. Blazek[146a], I. Bloch[45], C. Blocker[25],
A. Blue[56], W. Blum[86,*], U. Blumenschein[79], S. Blunier[34a], G.J. Bobbink[109],
V.S. Bobrovnikov[111,c], S.S. Bocchetta[84], A. Bocci[48], C. Bock[102], M. Boehler[51], D. Boerner[178],
D. Bogavac[102], A.G. Bogdanchikov[111], C. Bohm[148a], V. Boisvert[80], P. Bokan[168], T. Bold[41a],
A.S. Boldyrev[101], M. Bomben[83], M. Bona[79], M. Boonekamp[138], A. Borisov[132], G. Borissov[75],
J. Bortfeldt[32], D. Bortoletto[122], V. Bortolotto[62a,62b,62c], K. Bos[109], D. Boscherini[22a],
M. Bosman[13], J.D. Bossio Sola[29], J. Boudreau[127], J. Bouffard[2], E.V. Bouhova-Thacker[75],
D. Boumediene[37], C. Bourdarios[119], S.K. Boutle[56], A. Boveia[113], J. Boyd[32], I.R. Boyko[68],
J. Bracinik[19], A. Brandt[8], G. Brandt[57], O. Brandt[60a], U. Bratzler[158], B. Brau[89], J.E. Brau[118],
W.D. Breaden Madden[56], K. Brendlinger[45], A.J. Brennan[91], L. Brenner[109], R. Brenner[168],
S. Bressler[175], D.L. Briglin[19], T.M. Bristow[49], D. Britton[56], D. Britzger[45], F.M. Brochu[30],
I. Brock[23], R. Brock[93], G. Brooijmans[38], T. Brooks[80], W.K. Brooks[34b], J. Brosamer[16],
E. Brost[110], J.H Broughton[19], P.A. Bruckman de Renstrom[42], D. Bruncko[146b], A. Bruni[22a],
G. Bruni[22a], L.S. Bruni[109], BH Brunt[30], M. Bruschi[22a], N. Bruscino[23], P. Bryant[33],
L. Bryngemark[84], T. Buanes[15], Q. Buat[144], P. Buchholz[143], A.G. Buckley[56], I.A. Budagov[68],
F. Buehrer[51], M.K. Bugge[121], O. Bulekov[100], D. Bullock[8], H. Burckhart[32], S. Burdin[77],
C.D. Burgard[51], A.M. Burger[5], B. Burghgrave[110], K. Burka[42], S. Burke[133], I. Burmeister[46],
J.T.P. Burr[122], E. Busato[37], D. Büscher[51], V. Büscher[86], P. Bussey[56], J.M. Butler[24],
C.M. Buttar[56], J.M. Butterworth[81], P. Butti[109], W. Buttinger[27], A. Buzatu[35c],
A.R. Buzykaev[111,c], S. Cabrera Urbán[170], D. Caforio[130], V.M. Cairo[40a,40b], O. Cakir[4a],
N. Calace[52], P. Calafiura[16], A. Calandri[88], G. Calderini[83], P. Calfayan[64], G. Callea[40a,40b],
L.P. Caloba[26a], S. Calvente Lopez[85], D. Calvet[37], S. Calvet[37], T.P. Calvet[88], R. Camacho Toro[33],
S. Camarda[32], P. Camarri[135a,135b], D. Cameron[121], R. Caminal Armadans[169], C. Camincher[58],
S. Campana[32], M. Campanelli[81], A. Camplani[94a,94b], A. Campoverde[143], V. Canale[106a,106b],
M. Cano Bret[36c], J. Cantero[116], T. Cao[155], M.D.M. Capeans Garrido[32], I. Caprini[28b],
M. Caprini[28b], M. Capua[40a,40b], R.M. Carbone[38], R. Cardarelli[135a], F. Cardillo[51], I. Carli[131],
T. Carli[32], G. Carlino[106a], B.T. Carlson[127], L. Carminati[94a,94b], R.M.D. Carney[148a,148b],
S. Caron[108], E. Carquin[34b], G.D. Carrillo-Montoya[32], J. Carvalho[128a,128c], D. Casadei[19],
M.P. Casado[13,i], M. Casolino[13], D.W. Casper[166], R. Castelijn[109], A. Castelli[109],
V. Castillo Gimenez[170], N.F. Castro[128a,j], A. Catinaccio[32], J.R. Catmore[121], A. Cattai[32],
J. Caudron[23], V. Cavaliere[169], E. Cavallaro[13], D. Cavalli[94a], M. Cavalli-Sforza[13],
V. Cavasinni[126a,126b], E. Celebi[20a], F. Ceradini[136a,136b], L. Cerda Alberich[170], A.S. Cerqueira[26b],
A. Cerri[151], L. Cerrito[135a,135b], F. Cerutti[16], A. Cervelli[18], S.A. Cetin[20d], A. Chafaq[137a],
D. Chakraborty[110], S.K. Chan[59], W.S. Chan[109], Y.L. Chan[62a], P. Chang[169], J.D. Chapman[30],
D.G. Charlton[19], A. Chatterjee[52], C.C. Chau[161], C.A. Chavez Barajas[151], S. Che[113],
S. Cheatham[167a,167c], A. Chegwidden[93], S. Chekanov[6], S.V. Chekulaev[163a], G.A. Chelkov[68,k],
M.A. Chelstowska[32], C. Chen[67], H. Chen[27], S. Chen[35b], S. Chen[157], X. Chen[35c,l], Y. Chen[70],
H.C. Cheng[92], H.J. Cheng[35a], Y. Cheng[33], A. Cheplakov[68], E. Cheremushkina[132],
R. Cherkaoui El Moursli[137e], V. Chernyatin[27,*], E. Cheu[7], L. Chevalier[138], V. Chiarella[50],
G. Chiarelli[126a,126b], G. Chiodini[76a], A.S. Chisholm[32], A. Chitan[28b], Y.H. Chiu[172],
M.V. Chizhov[68], K. Choi[64], A.R. Chomont[37], S. Chouridou[9], B.K.B. Chow[102],
V. Christodoulou[81], D. Chromek-Burckhart[32], M.C. Chu[62a], J. Chudoba[129], A.J. Chuinard[90],
J.J. Chwastowski[42], L. Chytka[117], A.K. Ciftci[4a], D. Cinca[46], V. Cindro[78], I.A. Cioara[23],
C. Ciocca[22a,22b], A. Ciocio[16], F. Cirotto[106a,106b], Z.H. Citron[175], M. Citterio[94a], M. Ciubancan[28b],
A. Clark[52], B.L. Clark[59], M.R. Clark[38], P.J. Clark[49], R.N. Clarke[16], C. Clement[148a,148b],
Y. Coadou[88], M. Cobal[167a,167c], A. Coccaro[52], J. Cochran[67], L. Colasurdo[108], B. Cole[38],
A.P. Colijn[109], J. Collot[58], T. Colombo[166], P. Conde Muiño[128a,128b], E. Coniavitis[51],
S.H. Connell[147b], I.A. Connelly[87], V. Consorti[51], S. Constantinescu[28b], G. Conti[32],

F. Conventi[106a,m], M. Cooke[16], B.D. Cooper[81], A.M. Cooper-Sarkar[122], F. Cormier[171],
K.J.R. Cormier[161], T. Cornelissen[178], M. Corradi[134a,134b], F. Corriveau[90,n], A. Cortes-Gonzalez[32],
G. Cortiana[103], G. Costa[94a], M.J. Costa[170], D. Costanzo[141], G. Cottin[30], G. Cowan[80],
B.E. Cox[87], K. Cranmer[112], S.J. Crawley[56], R.A. Creager[124], G. Cree[31], S. Crépé-Renaudin[58],
F. Crescioli[83], W.A. Cribbs[148a,148b], M. Crispin Ortuzar[122], M. Cristinziani[23], V. Croft[108],
G. Crosetti[40a,40b], A. Cueto[85], T. Cuhadar Donszelmann[141], J. Cummings[179], M. Curatolo[50],
J. Cúth[86], H. Czirr[143], P. Czodrowski[32], G. D'amen[22a,22b], S. D'Auria[56], M. D'Onofrio[77],
M.J. Da Cunha Sargedas De Sousa[128a,128b], C. Da Via[87], W. Dabrowski[41a], T. Dado[146a],
T. Dai[92], O. Dale[15], F. Dallaire[97], C. Dallapiccola[89], M. Dam[39], J.R. Dandoy[124], N.P. Dang[51],
A.C. Daniells[19], N.S. Dann[87], M. Danninger[171], M. Dano Hoffmann[138], V. Dao[150], G. Darbo[53a],
S. Darmora[8], J. Dassoulas[3], A. Dattagupta[118], T. Daubney[45], W. Davey[23], C. David[45],
T. Davidek[131], M. Davies[155], P. Davison[81], E. Dawe[91], I. Dawson[141], K. De[8], R. de Asmundis[106a],
A. De Benedetti[115], S. De Castro[22a,22b], S. De Cecco[83], N. De Groot[108], P. de Jong[109],
H. De la Torre[93], F. De Lorenzi[67], A. De Maria[57], D. De Pedis[134a], A. De Salvo[134a],
U. De Sanctis[151], A. De Santo[151], K. De Vasconcelos Corga[88], J.B. De Vivie De Regie[119],
W.J. Dearnaley[75], R. Debbe[27], C. Debenedetti[139], D.V. Dedovich[68], N. Dehghanian[3],
I. Deigaard[109], M. Del Gaudio[40a,40b], J. Del Peso[85], T. Del Prete[126a,126b], D. Delgove[119],
F. Deliot[138], C.M. Delitzsch[52], A. Dell'Acqua[32], L. Dell'Asta[24], M. Dell'Orso[126a,126b],
M. Della Pietra[106a,m], D. della Volpe[52], M. Delmastro[5], P.A. Delsart[58], D.A. DeMarco[161],
S. Demers[179], M. Demichev[68], A. Demilly[83], S.P. Denisov[132], D. Denysiuk[138], D. Derendarz[42],
J.E. Derkaoui[137d], F. Derue[83], P. Dervan[77], K. Desch[23], C. Deterre[45], K. Dette[46],
P.O. Deviveiros[32], A. Dewhurst[133], S. Dhaliwal[25], A. Di Ciaccio[135a,135b], L. Di Ciaccio[5],
W.K. Di Clemente[124], C. Di Donato[106a,106b], A. Di Girolamo[32], B. Di Girolamo[32],
B. Di Micco[136a,136b], R. Di Nardo[32], K.F. Di Petrillo[59], A. Di Simone[51], R. Di Sipio[161],
D. Di Valentino[31], C. Diaconu[88], M. Diamond[161], F.A. Dias[49], M.A. Diaz[34a], E.B. Diehl[92],
J. Dietrich[17], S. Díez Cornell[45], A. Dimitrievska[14], J. Dingfelder[23], P. Dita[28b], S. Dita[28b],
F. Dittus[32], F. Djama[88], T. Djobava[54b], J.I. Djuvsland[60a], M.A.B. do Vale[26c], D. Dobos[32],
M. Dobre[28b], C. Doglioni[84], J. Dolejsi[131], Z. Dolezal[131], M. Donadelli[26d], S. Donati[126a,126b],
P. Dondero[123a,123b], J. Donini[37], J. Dopke[133], A. Doria[106a], M.T. Dova[74], A.T. Doyle[56],
E. Drechsler[57], M. Dris[10], Y. Du[36b], J. Duarte-Campderros[155], E. Duchovni[175], G. Duckeck[102],
O.A. Ducu[97,o], D. Duda[109], A. Dudarev[32], A.Chr. Dudder[86], E.M. Duffield[16], L. Duflot[119],
M. Dührssen[32], M. Dumancic[175], A.E. Dumitriu[28b], A.K. Duncan[56], M. Dunford[60a],
H. Duran Yildiz[4a], M. Düren[55], A. Durglishvili[54b], D. Duschinger[47], B. Dutta[45], M. Dyndal[45],
C. Eckardt[45], K.M. Ecker[103], R.C. Edgar[92], T. Eifert[32], G. Eigen[15], K. Einsweiler[16], T. Ekelof[168],
M. El Kacimi[137c], V. Ellajosyula[88], M. Ellert[168], S. Elles[5], F. Ellinghaus[178], A.A. Elliot[172],
N. Ellis[32], J. Elmsheuser[27], M. Elsing[32], D. Emeliyanov[133], Y. Enari[157], O.C. Endner[86],
J.S. Ennis[173], J. Erdmann[46], A. Ereditato[18], G. Ernis[178], M. Ernst[27], S. Errede[169], E. Ertel[86],
M. Escalier[119], H. Esch[46], C. Escobar[127], B. Esposito[50], A.I. Etienvre[138], E. Etzion[155],
H. Evans[64], A. Ezhilov[125], M. Ezzi[137e], F. Fabbri[22a,22b], L. Fabbri[22a,22b], G. Facini[33],
R.M. Fakhrutdinov[132], S. Falciano[134a], R.J. Falla[81], J. Faltova[32], Y. Fang[35a], M. Fanti[94a,94b],
A. Farbin[8], A. Farilla[136a], C. Farina[127], E.M. Farina[123a,123b], T. Farooque[93], S. Farrell[16],
S.M. Farrington[173], P. Farthouat[32], F. Fassi[137e], P. Fassnacht[32], D. Fassouliotis[9],
M. Faucci Giannelli[80], A. Favareto[53a,53b], W.J. Fawcett[122], L. Fayard[119], O.L. Fedin[125,p],
W. Fedorko[171], S. Feigl[121], L. Feligioni[88], C. Feng[36b], E.J. Feng[32], H. Feng[92], A.B. Fenyuk[132],
L. Feremenga[8], P. Fernandez Martinez[170], S. Fernandez Perez[13], J. Ferrando[45], A. Ferrari[168],
P. Ferrari[109], R. Ferrari[123a], D.E. Ferreira de Lima[60b], A. Ferrer[170], D. Ferrere[52], C. Ferretti[92],
F. Fiedler[86], A. Filipčič[78], M. Filipuzzi[45], F. Filthaut[108], M. Fincke-Keeler[172], K.D. Finelli[152],
M.C.N. Fiolhais[128a,128c], L. Fiorini[170], A. Fischer[2], C. Fischer[13], J. Fischer[178], W.C. Fisher[93],

N. Flaschel[45], I. Fleck[143], P. Fleischmann[92], R.R.M. Fletcher[124], T. Flick[178], B.M. Flierl[102],
L.R. Flores Castillo[62a], M.J. Flowerdew[103], G.T. Forcolin[87], A. Formica[138], A. Forti[87],
A.G. Foster[19], D. Fournier[119], H. Fox[75], S. Fracchia[13], P. Francavilla[83], M. Franchini[22a,22b],
D. Francis[32], L. Franconi[121], M. Franklin[59], M. Frate[166], M. Fraternali[123a,123b], D. Freeborn[81],
S.M. Fressard-Batraneanu[32], B. Freund[97], D. Froidevaux[32], J.A. Frost[122], C. Fukunaga[158],
E. Fullana Torregrosa[86], T. Fusayasu[104], J. Fuster[170], C. Gabaldon[58], O. Gabizon[154],
A. Gabrielli[22a,22b], A. Gabrielli[16], G.P. Gach[41a], S. Gadatsch[32], S. Gadomski[80],
G. Gagliardi[53a,53b], L.G. Gagnon[97], P. Gagnon[64], C. Galea[108], B. Galhardo[128a,128c],
E.J. Gallas[122], B.J. Gallop[133], P. Gallus[130], G. Galster[39], K.K. Gan[113], S. Ganguly[37], J. Gao[36a],
Y. Gao[77], Y.S. Gao[145,g], F.M. Garay Walls[49], C. García[170], J.E. García Navarro[170],
M. Garcia-Sciveres[16], R.W. Gardner[33], N. Garelli[145], V. Garonne[121], A. Gascon Bravo[45],
K. Gasnikova[45], C. Gatti[50], A. Gaudiello[53a,53b], G. Gaudio[123a], I.L. Gavrilenko[98], C. Gay[171],
G. Gaycken[23], E.N. Gazis[10], C.N.P. Gee[133], M. Geisen[86], M.P. Geisler[60a], K. Gellerstedt[148a,148b],
C. Gemme[53a], M.H. Genest[58], C. Geng[36a,q], S. Gentile[134a,134b], C. Gentsos[156], S. George[80],
D. Gerbaudo[13], A. Gershon[155], S. Ghasemi[143], M. Ghneimat[23], B. Giacobbe[22a], S. Giagu[134a,134b],
P. Giannetti[126a,126b], S.M. Gibson[80], M. Gignac[171], M. Gilchriese[16], D. Gillberg[31], G. Gilles[178],
D.M. Gingrich[3,d], N. Giokaris[9,*], M.P. Giordani[167a,167c], F.M. Giorgi[22a], P.F. Giraud[138],
P. Giromini[59], D. Giugni[94a], F. Giuli[122], C. Giuliani[103], M. Giulini[60b], B.K. Gjelsten[121],
S. Gkaitatzis[156], I. Gkialas[9], E.L. Gkougkousis[139], L.K. Gladilin[101], C. Glasman[85], J. Glatzer[13],
P.C.F. Glaysher[45], A. Glazov[45], M. Goblirsch-Kolb[25], J. Godlewski[42], S. Goldfarb[91], T. Golling[52],
D. Golubkov[132], A. Gomes[128a,128b,128d], R. Gonçalo[128a], R. Goncalves Gama[26a],
J. Goncalves Pinto Firmino Da Costa[138], G. Gonella[51], L. Gonella[19], A. Gongadze[68],
S. González de la Hoz[170], S. Gonzalez-Sevilla[52], L. Goossens[32], P.A. Gorbounov[99],
H.A. Gordon[27], I. Gorelov[107], B. Gorini[32], E. Gorini[76a,76b], A. Gorišek[78], A.T. Goshaw[48],
C. Gössling[46], M.I. Gostkin[68], C.R. Goudet[119], D. Goujdami[137c], A.G. Goussiou[140],
N. Govender[147b,r], E. Gozani[154], L. Graber[57], I. Grabowska-Bold[41a], P.O.J. Gradin[58],
J. Gramling[52], E. Gramstad[121], S. Grancagnolo[17], V. Gratchev[125], P.M. Gravila[28f], H.M. Gray[32],
Z.D. Greenwood[82,s], C. Grefe[23], K. Gregersen[81], I.M. Gregor[45], P. Grenier[145], K. Grevtsov[5],
J. Griffiths[8], A.A. Grillo[139], K. Grimm[75], S. Grinstein[13,t], Ph. Gris[37], J.-F. Grivaz[119], S. Groh[86],
E. Gross[175], J. Grosse-Knetter[57], G.C. Grossi[82], Z.J. Grout[81], L. Guan[92], W. Guan[176],
J. Guenther[65], F. Guescini[163a], D. Guest[166], O. Gueta[155], B. Gui[113], E. Guido[53a,53b],
T. Guillemin[5], S. Guindon[2], U. Gul[56], C. Gumpert[32], J. Guo[36c], W. Guo[92], Y. Guo[36a],
R. Gupta[43], S. Gupta[122], G. Gustavino[134a,134b], P. Gutierrez[115], N.G. Gutierrez Ortiz[81],
C. Gutschow[81], C. Guyot[138], M.P. Guzik[41a], C. Gwenlan[122], C.B. Gwilliam[77], A. Haas[112],
C. Haber[16], H.K. Hadavand[8], N. Haddad[137e], A. Hadef[88], S. Hageböck[23], M. Hagihara[164],
H. Hakobyan[180,*], M. Haleem[45], J. Haley[116], G. Halladjian[93], G.D. Hallewell[88], K. Hamacher[178],
P. Hamal[117], K. Hamano[172], A. Hamilton[147a], G.N. Hamity[141], P.G. Hamnett[45], L. Han[36a],
S. Han[35a], K. Hanagaki[69,u], K. Hanawa[157], M. Hance[139], B. Haney[124], P. Hanke[60a], R. Hanna[138],
J.B. Hansen[39], J.D. Hansen[39], M.C. Hansen[23], P.H. Hansen[39], K. Hara[164], A.S. Hard[176],
T. Harenberg[178], F. Hariri[119], S. Harkusha[95], R.D. Harrington[49], P.F. Harrison[173], F. Hartjes[109],
N.M. Hartmann[102], M. Hasegawa[70], Y. Hasegawa[142], A. Hasib[49], S. Hassani[138], S. Haug[18],
R. Hauser[93], L. Hauswald[47], L.B. Havener[38], M. Havranek[130], C.M. Hawkes[19], R.J. Hawkings[32],
D. Hayakawa[159], D. Hayden[93], C.P. Hays[122], J.M. Hays[79], H.S. Hayward[77], S.J. Haywood[133],
S.J. Head[19], T. Heck[86], V. Hedberg[84], L. Heelan[8], S. Heim[45], T. Heim[16], B. Heinemann[45,v],
J.J. Heinrich[102], L. Heinrich[112], C. Heinz[55], J. Hejbal[129], L. Helary[32], A. Held[171],
S. Hellman[148a,148b], C. Helsens[32], J. Henderson[122], R.C.W. Henderson[75], Y. Heng[176],
S. Henkelmann[171], A.M. Henriques Correia[32], S. Henrot-Versille[119], G.H. Herbert[17], H. Herde[25],
V. Herget[177], Y. Hernández Jiménez[147c], G. Herten[51], R. Hertenberger[102], L. Hervas[32],

T.C. Herwig[124], G.G. Hesketh[81], N.P. Hessey[109], J.W. Hetherly[43], S. Higashino[69],
E. Higón-Rodriguez[170], E. Hill[172], J.C. Hill[30], K.H. Hiller[45], S.J. Hillier[19], I. Hinchliffe[16],
M. Hirose[51], D. Hirschbuehl[178], B. Hiti[78], O. Hladik[129], X. Hoad[49], J. Hobbs[150], N. Hod[163a],
M.C. Hodgkinson[141], P. Hodgson[141], A. Hoecker[32], M.R. Hoeferkamp[107], F. Hoenig[102],
D. Hohn[23], T.R. Holmes[16], M. Homann[46], S. Honda[164], T. Honda[69], T.M. Hong[127],
B.H. Hooberman[169], W.H. Hopkins[118], Y. Horii[105], A.J. Horton[144], J-Y. Hostachy[58], S. Hou[153],
A. Hoummada[137a], J. Howarth[45], J. Hoya[74], M. Hrabovsky[117], I. Hristova[17], J. Hrivnac[119],
T. Hryn'ova[5], A. Hrynevich[96], P.J. Hsu[63], S.-C. Hsu[140], Q. Hu[36a], S. Hu[36c], Y. Huang[35a],
Z. Hubacek[130], F. Hubaut[88], F. Huegging[23], T.B. Huffman[122], E.W. Hughes[38], G. Hughes[75],
M. Huhtinen[32], P. Huo[150], N. Huseynov[68,b], J. Huston[93], J. Huth[59], G. Iacobucci[52],
G. Iakovidis[27], I. Ibragimov[143], L. Iconomidou-Fayard[119], Z. Idrissi[137e], P. Iengo[32],
O. Igonkina[109,w], T. Iizawa[174], Y. Ikegami[69], M. Ikeno[69], Y. Ilchenko[11,x], D. Iliadis[156], N. Ilic[145],
G. Introzzi[123a,123b], P. Ioannou[9,*], M. Iodice[136a], K. Iordanidou[38], V. Ippolito[59], N. Ishijima[120],
M. Ishino[157], M. Ishitsuka[159], C. Issever[122], S. Istin[20a], F. Ito[164], J.M. Iturbe Ponce[87],
R. Iuppa[162a,162b], H. Iwasaki[69], J.M. Izen[44], V. Izzo[106a], S. Jabbar[3], P. Jackson[1], V. Jain[2],
K.B. Jakobi[86], K. Jakobs[51], S. Jakobsen[32], T. Jakoubek[129], D.O. Jamin[116], D.K. Jana[82],
R. Jansky[65], J. Janssen[23], M. Janus[57], P.A. Janus[41a], G. Jarlskog[84], N. Javadov[68,b], T. Javůrek[51],
M. Javurkova[51], F. Jeanneau[138], L. Jeanty[16], J. Jejelava[54a,y], A. Jelinskas[173], P. Jenni[51,z],
C. Jeske[173], S. Jézéquel[5], H. Ji[176], J. Jia[150], H. Jiang[67], Y. Jiang[36a], Z. Jiang[145], S. Jiggins[81],
J. Jimenez Pena[170], S. Jin[35a], A. Jinaru[28b], O. Jinnouchi[159], H. Jivan[147c], P. Johansson[141],
K.A. Johns[7], C.A. Johnson[64], W.J. Johnson[140], K. Jon-And[148a,148b], R.W.L. Jones[75], S. Jones[7],
T.J. Jones[77], J. Jongmanns[60a], P.M. Jorge[128a,128b], J. Jovicevic[163a], X. Ju[176], A. Juste Rozas[13,t],
M.K. Köhler[175], A. Kaczmarska[42], M. Kado[119], H. Kagan[113], M. Kagan[145], S.J. Kahn[88],
T. Kaji[174], E. Kajomovitz[48], C.W. Kalderon[84], A. Kaluza[86], S. Kama[43], A. Kamenshchikov[132],
N. Kanaya[157], S. Kaneti[30], L. Kanjir[78], V.A. Kantserov[100], J. Kanzaki[69], B. Kaplan[112],
L.S. Kaplan[176], D. Kar[147c], K. Karakostas[10], N. Karastathis[10], M.J. Kareem[57], E. Karentzos[10],
S.N. Karpov[68], Z.M. Karpova[68], K. Karthik[112], V. Kartvelishvili[75], A.N. Karyukhin[132],
K. Kasahara[164], L. Kashif[176], R.D. Kass[113], A. Kastanas[149], Y. Kataoka[157], C. Kato[157],
A. Katre[52], J. Katzy[45], K. Kawade[105], K. Kawagoe[73], T. Kawamoto[157], G. Kawamura[57],
V.F. Kazanin[111,c], R. Keeler[172], R. Kehoe[43], J.S. Keller[45], J.J. Kempster[80], H. Keoshkerian[161],
O. Kepka[129], B.P. Kerševan[78], S. Kersten[178], R.A. Keyes[90], M. Khader[169], F. Khalil-zada[12],
A. Khanov[116], A.G. Kharlamov[111,c], T. Kharlamova[111,c], A. Khodinov[160], T.J. Khoo[52],
V. Khovanskiy[99], E. Khramov[68], J. Khubua[54b,aa], S. Kido[70], C.R. Kilby[80], H.Y. Kim[8],
S.H. Kim[164], Y.K. Kim[33], N. Kimura[156], O.M. Kind[17], B.T. King[77], D. Kirchmeier[47], J. Kirk[133],
A.E. Kiryunin[103], T. Kishimoto[157], D. Kisielewska[41a], K. Kiuchi[164], O. Kivernyk[138],
E. Kladiva[146b], T. Klapdor-kleingrothaus[51], M.H. Klein[38], M. Klein[77], U. Klein[77],
K. Kleinknecht[86], P. Klimek[110], A. Klimentov[27], R. Klingenberg[46], T. Klioutchnikova[32],
E.-E. Kluge[60a], P. Kluit[109], S. Kluth[103], J. Knapik[42], E. Kneringer[65], E.B.F.G. Knoops[88],
A. Knue[103], A. Kobayashi[157], D. Kobayashi[159], T. Kobayashi[157], M. Kobel[47], M. Kocian[145],
P. Kodys[131], T. Koffas[31], E. Koffeman[109], N.M. Köhler[103], T. Koi[145], M. Kolb[60b], I. Koletsou[5],
A.A. Komar[98,*], Y. Komori[157], T. Kondo[69], N. Kondrashova[36c], K. Köneke[51], A.C. König[108],
T. Kono[69,ab], R. Konoplich[112,ac], N. Konstantinidis[81], R. Kopeliansky[64], S. Koperny[41a],
A.K. Kopp[51], K. Korcyl[42], K. Kordas[156], A. Korn[81], A.A. Korol[111,c], I. Korolkov[13],
E.V. Korolkova[141], O. Kortner[103], S. Kortner[103], T. Kosek[131], V.V. Kostyukhin[23], A. Kotwal[48],
A. Koulouris[10], A. Kourkoumeli-Charalampidi[123a,123b], C. Kourkoumelis[9], V. Kouskoura[27],
A.B. Kowalewska[42], R. Kowalewski[172], T.Z. Kowalski[41a], C. Kozakai[157], W. Kozanecki[138],
A.S. Kozhin[132], V.A. Kramarenko[101], G. Kramberger[78], D. Krasnopevtsev[100], M.W. Krasny[83],
A. Krasznahorkay[32], A. Kravchenko[27], J.A. Kremer[41a], M. Kretz[60c], J. Kretzschmar[77],

K. Kreutzfeldt[55], P. Krieger[161], K. Krizka[33], K. Kroeninger[46], H. Kroha[103], J. Kroll[124],
J. Kroseberg[23], J. Krstic[14], U. Kruchonak[68], H. Krüger[23], N. Krumnack[67], M.C. Kruse[48],
M. Kruskal[24], T. Kubota[91], H. Kucuk[81], S. Kuday[4b], J.T. Kuechler[178], S. Kuehn[51], A. Kugel[60c],
F. Kuger[177], T. Kuhl[45], V. Kukhtin[68], R. Kukla[88], Y. Kulchitsky[95], S. Kuleshov[34b],
Y.P. Kulinich[169], M. Kuna[134a,134b], T. Kunigo[71], A. Kupco[129], O. Kuprash[155], H. Kurashige[70],
L.L. Kurchaninov[163a], Y.A. Kurochkin[95], M.G. Kurth[35a], V. Kus[129], E.S. Kuwertz[172],
M. Kuze[159], J. Kvita[117], T. Kwan[172], D. Kyriazopoulos[141], A. La Rosa[103],
J.L. La Rosa Navarro[26d], L. La Rotonda[40a,40b], C. Lacasta[170], F. Lacava[134a,134b], J. Lacey[45],
H. Lacker[17], D. Lacour[83], E. Ladygin[68], R. Lafaye[5], B. Laforge[83], T. Lagouri[179], S. Lai[57],
S. Lammers[64], W. Lampl[7], E. Lançon[27], U. Landgraf[51], M.P.J. Landon[79], M.C. Lanfermann[52],
V.S. Lang[60a], J.C. Lange[13], A.J. Lankford[166], F. Lanni[27], K. Lantzsch[23], A. Lanza[123a],
A. Lapertosa[53a,53b], S. Laplace[83], J.F. Laporte[138], T. Lari[94a], F. Lasagni Manghi[22a,22b],
M. Lassnig[32], P. Laurelli[50], W. Lavrijsen[16], A.T. Law[139], P. Laycock[77], T. Lazovich[59],
M. Lazzaroni[94a,94b], B. Le[91], O. Le Dortz[83], E. Le Guirriec[88], E.P. Le Quilleuc[138], M. LeBlanc[172],
T. LeCompte[6], F. Ledroit-Guillon[58], C.A. Lee[27], S.C. Lee[153], L. Lee[1], B. Lefebvre[90],
G. Lefebvre[83], M. Lefebvre[172], F. Legger[102], C. Leggett[16], A. Lehan[77], G. Lehmann Miotto[32],
X. Lei[7], W.A. Leight[45], A.G. Leister[179], M.A.L. Leite[26d], R. Leitner[131], D. Lellouch[175],
B. Lemmer[57], K.J.C. Leney[81], T. Lenz[23], B. Lenzi[32], R. Leone[7], S. Leone[126a,126b],
C. Leonidopoulos[49], G. Lerner[151], C. Leroy[97], A.A.J. Lesage[138], C.G. Lester[30], M. Levchenko[125],
J. Levêque[5], D. Levin[92], L.J. Levinson[175], M. Levy[19], D. Lewis[79], M. Leyton[44], B. Li[36a,q],
C. Li[36a], H. Li[150], L. Li[48], L. Li[36c], Q. Li[35a], S. Li[48], X. Li[36c], Y. Li[143], Z. Liang[35a], B. Liberti[135a],
A. Liblong[161], K. Lie[169], J. Liebal[23], W. Liebig[15], A. Limosani[152], S.C. Lin[153,ad], T.H. Lin[86],
B.E. Lindquist[150], A.E. Lionti[52], E. Lipeles[124], A. Lipniacka[15], M. Lisovyi[60b], T.M. Liss[169],
A. Lister[171], A.M. Litke[139], B. Liu[153,ae], H. Liu[92], H. Liu[27], J. Liu[36b], J.B. Liu[36a], K. Liu[88],
L. Liu[169], M. Liu[36a], Y.L. Liu[36a], Y. Liu[36a], M. Livan[123a,123b], A. Lleres[58], J. Llorente Merino[35a],
S.L. Lloyd[79], C.Y. Lo[62b], F. Lo Sterzo[153], E.M. Lobodzinska[45], P. Loch[7], F.K. Loebinger[87],
K.M. Loew[25], A. Loginov[179,*], T. Lohse[17], K. Lohwasser[45], M. Lokajicek[129], B.A. Long[24],
J.D. Long[169], R.E. Long[75], L. Longo[76a,76b], K.A. Looper[113], J.A. Lopez[34b], D. Lopez Mateos[59],
I. Lopez Paz[13], A. Lopez Solis[83], J. Lorenz[102], N. Lorenzo Martinez[64], M. Losada[21], P.J. Lösel[102],
X. Lou[35a], A. Lounis[119], J. Love[6], P.A. Love[75], H. Lu[62a], N. Lu[92], Y. Lu[63], H.J. Lubatti[140],
C. Luci[134a,134b], A. Lucotte[58], C. Luedtke[51], F. Luehring[64], W. Lukas[65], L. Luminari[134a],
O. Lundberg[148a,148b], B. Lund-Jensen[149], P.M. Luzi[83], D. Lynn[27], R. Lysak[129], E. Lytken[84],
V. Lyubushkin[68], H. Ma[27], L.L. Ma[36b], Y. Ma[36b], G. Maccarrone[50], A. Macchiolo[103],
C.M. Macdonald[141], B. Maček[78], J. Machado Miguens[124,128b], D. Madaffari[88], R. Madar[37],
H.J. Maddocks[168], W.F. Mader[47], A. Madsen[45], J. Maeda[70], S. Maeland[15], T. Maeno[27],
A. Maevskiy[101], E. Magradze[57], J. Mahlstedt[109], C. Maiani[119], C. Maidantchik[26a], A.A. Maier[103],
T. Maier[102], A. Maio[128a,128b,128d], S. Majewski[118], Y. Makida[69], N. Makovec[119], B. Malaescu[83],
Pa. Malecki[42], V.P. Maleev[125], F. Malek[58], U. Mallik[66], D. Malon[6], C. Malone[30], S. Maltezos[10],
S. Malyukov[32], J. Mamuzic[170], G. Mancini[50], L. Mandelli[94a], I. Mandić[78], J. Maneira[128a,128b],
L. Manhaes de Andrade Filho[26b], J. Manjarres Ramos[163b], A. Mann[102], A. Manousos[32],
B. Mansoulie[138], J.D. Mansour[35a], R. Mantifel[90], M. Mantoani[57], S. Manzoni[94a,94b], L. Mapelli[32],
G. Marceca[29], L. March[52], G. Marchiori[83], M. Marcisovsky[129], M. Marjanovic[37], D.E. Marley[92],
F. Marroquim[26a], S.P. Marsden[87], Z. Marshall[16], M.U.F Martensson[168], S. Marti-Garcia[170],
C.B. Martin[113], T.A. Martin[173], V.J. Martin[49], B. Martin dit Latour[15], M. Martinez[13,t],
V.I. Martinez Outschoorn[169], S. Martin-Haugh[133], V.S. Martoiu[28b], A.C. Martyniuk[81],
A. Marzin[115], L. Masetti[86], T. Mashimo[157], R. Mashinistov[98], J. Masik[87], A.L. Maslennikov[111,c],
L. Massa[135a,135b], P. Mastrandrea[5], A. Mastroberardino[40a,40b], T. Masubuchi[157], P. Mättig[178],
J. Maurer[28b], S.J. Maxfield[77], D.A. Maximov[111,c], R. Mazini[153], I. Maznas[156], S.M. Mazza[94a,94b],

N.C. Mc Fadden[107], G. Mc Goldrick[161], S.P. Mc Kee[92], A. McCarn[92], R.L. McCarthy[150],
T.G. McCarthy[103], L.I. McClymont[81], E.F. McDonald[91], J.A. Mcfayden[81], G. Mchedlidze[57],
S.J. McMahon[133], P.C. McNamara[91], R.A. McPherson[172,n], S. Meehan[140], T.J. Megy[51],
S. Mehlhase[102], A. Mehta[77], T. Meideck[58], K. Meier[60a], C. Meineck[102], B. Meirose[44],
D. Melini[170,af], B.R. Mellado Garcia[147c], M. Melo[146a], F. Meloni[18], S.B. Menary[87], L. Meng[77],
X.T. Meng[92], A. Mengarelli[22a,22b], S. Menke[103], E. Meoni[165], S. Mergelmeyer[17], P. Mermod[52],
L. Merola[106a,106b], C. Meroni[94a], F.S. Merritt[33], A. Messina[134a,134b], J. Metcalfe[6], A.S. Mete[166],
C. Meyer[124], J-P. Meyer[138], J. Meyer[109], H. Meyer Zu Theenhausen[60a], F. Miano[151],
R.P. Middleton[133], S. Miglioranzi[53a,53b], L. Mijović[49], G. Mikenberg[175], M. Mikestikova[129],
M. Mikuž[78], M. Milesi[91], A. Milic[27], D.W. Miller[33], C. Mills[49], A. Milov[175],
D.A. Milstead[148a,148b], A.A. Minaenko[132], Y. Minami[157], I.A. Minashvili[68], A.I. Mincer[112],
B. Mindur[41a], M. Mineev[68], Y. Minegishi[157], Y. Ming[176], L.M. Mir[13], K.P. Mistry[124],
T. Mitani[174], J. Mitrevski[102], V.A. Mitsou[170], A. Miucci[18], P.S. Miyagawa[141], A. Mizukami[69],
J.U. Mjörnmark[84], M. Mlynarikova[131], T. Moa[148a,148b], K. Mochizuki[97], P. Mogg[51],
S. Mohapatra[38], S. Molander[148a,148b], R. Moles-Valls[23], R. Monden[71], M.C. Mondragon[93],
K. Mönig[45], J. Monk[39], E. Monnier[88], A. Montalbano[150], J. Montejo Berlingen[32], F. Monticelli[74],
S. Monzani[94a,94b], R.W. Moore[3], N. Morange[119], D. Moreno[21], M. Moreno Llácer[57],
P. Morettini[53a], S. Morgenstern[32], D. Mori[144], T. Mori[157], M. Morii[59], M. Morinaga[157],
V. Morisbak[121], A.K. Morley[152], G. Mornacchi[32], J.D. Morris[79], L. Morvaj[150], P. Moschovakos[10],
M. Mosidze[54b], H.J. Moss[141], J. Moss[145,ag], K. Motohashi[159], R. Mount[145], E. Mountricha[27],
E.J.W. Moyse[89], S. Muanza[88], R.D. Mudd[19], F. Mueller[103], J. Mueller[127], R.S.P. Mueller[102],
D. Muenstermann[75], P. Mullen[56], G.A. Mullier[18], F.J. Munoz Sanchez[87], W.J. Murray[173,133],
H. Musheghyan[57], M. Muškinja[78], A.G. Myagkov[132,ah], M. Myska[130], B.P. Nachman[16],
O. Nackenhorst[52], K. Nagai[122], R. Nagai[69,ab], K. Nagano[69], Y. Nagasaka[61], K. Nagata[164],
M. Nagel[51], E. Nagy[88], A.M. Nairz[32], Y. Nakahama[105], K. Nakamura[69], T. Nakamura[157],
I. Nakano[114], R.F. Naranjo Garcia[45], R. Narayan[11], D.I. Narrias Villar[60a], I. Naryshkin[125],
T. Naumann[45], G. Navarro[21], R. Nayyar[7], H.A. Neal[92], P.Yu. Nechaeva[98], T.J. Neep[138],
A. Negri[123a,123b], M. Negrini[22a], S. Nektarijevic[108], C. Nellist[119], A. Nelson[166], S. Nemecek[129],
P. Nemethy[112], A.A. Nepomuceno[26a], M. Nessi[32,ai], M.S. Neubauer[169], M. Neumann[178],
R.M. Neves[112], P. Nevski[27], P.R. Newman[19], T.Y. Ng[62c], T. Nguyen Manh[97], R.B. Nickerson[122],
R. Nicolaidou[138], J. Nielsen[139], V. Nikolaenko[132,ah], I. Nikolic-Audit[83], K. Nikolopoulos[19],
J.K. Nilsen[121], P. Nilsson[27], Y. Ninomiya[157], A. Nisati[134a], N. Nishu[35c], R. Nisius[103], T. Nobe[157],
Y. Noguchi[71], M. Nomachi[120], I. Nomidis[31], M.A. Nomura[27], T. Nooney[79], M. Nordberg[32],
N. Norjoharuddeen[122], O. Novgorodova[47], S. Nowak[103], M. Nozaki[69], L. Nozka[117], K. Ntekas[166],
E. Nurse[81], F. Nuti[91], D.C. O'Neil[144], A.A. O'Rourke[45], V. O'Shea[56], F.G. Oakham[31,d],
H. Oberlack[103], T. Obermann[23], J. Ocariz[83], A. Ochi[70], I. Ochoa[38], J.P. Ochoa-Ricoux[34a],
S. Oda[73], S. Odaka[69], H. Ogren[64], A. Oh[87], S.H. Oh[48], C.C. Ohm[16], H. Ohman[168], H. Oide[53a,53b],
H. Okawa[164], Y. Okumura[157], T. Okuyama[69], A. Olariu[28b], L.F. Oleiro Seabra[128a],
S.A. Olivares Pino[49], D. Oliveira Damazio[27], A. Olszewski[42], J. Olszowska[42], A. Onofre[128a,128e],
K. Onogi[105], P.U.E. Onyisi[11,x], M.J. Oreglia[33], Y. Oren[155], D. Orestano[136a,136b], N. Orlando[62b],
R.S. Orr[161], B. Osculati[53a,53b,*], R. Ospanov[87], G. Otero y Garzon[29], H. Otono[73], M. Ouchrif[137d],
F. Ould-Saada[121], A. Ouraou[138], K.P. Oussoren[109], Q. Ouyang[35a], M. Owen[56], R.E. Owen[19],
V.E. Ozcan[20a], N. Ozturk[8], K. Pachal[144], A. Pacheco Pages[13], L. Pacheco Rodriguez[138],
C. Padilla Aranda[13], S. Pagan Griso[16], M. Paganini[179], M. Paige[27], P. Pais[89], G. Palacino[64],
S. Palazzo[40a,40b], S. Palestini[32], M. Palka[41b], D. Pallin[37], E.St. Panagiotopoulou[10],
I. Panagoulias[10], C.E. Pandini[83], J.G. Panduro Vazquez[80], P. Pani[32], S. Panitkin[27], D. Pantea[28b],
L. Paolozzi[52], Th.D. Papadopoulou[10], K. Papageorgiou[9], A. Paramonov[6],
D. Paredes Hernandez[179], A.J. Parker[75], M.A. Parker[30], K.A. Parker[45], F. Parodi[53a,53b],

J.A. Parsons[38], U. Parzefall[51], V.R. Pascuzzi[161], J.M. Pasner[139], E. Pasqualucci[134a],
S. Passaggio[53a], Fr. Pastore[80], S. Pataraia[178], J.R. Pater[87], T. Pauly[32], J. Pearce[172],
B. Pearson[115], L.E. Pedersen[39], S. Pedraza Lopez[170], R. Pedro[128a,128b], S.V. Peleganchuk[111,c],
O. Penc[129], C. Peng[35a], H. Peng[36a], J. Penwell[64], B.S. Peralva[26b], M.M. Perego[138],
D.V. Perepelitsa[27], L. Perini[94a,94b], H. Pernegger[32], S. Perrella[106a,106b], R. Peschke[45],
V.D. Peshekhonov[68], K. Peters[45], R.F.Y. Peters[87], B.A. Petersen[32], T.C. Petersen[39], E. Petit[58],
A. Petridis[1], C. Petridou[156], P. Petroff[119], E. Petrolo[134a], M. Petrov[122], F. Petrucci[136a,136b],
N.E. Pettersson[89], A. Peyaud[138], R. Pezoa[34b], P.W. Phillips[133], G. Piacquadio[150], E. Pianori[173],
A. Picazio[89], E. Piccaro[79], M.A. Pickering[122], R. Piegaia[29], J.E. Pilcher[33], A.D. Pilkington[87],
A.W.J. Pin[87], M. Pinamonti[167a,167c,aj], J.L. Pinfold[3], H. Pirumov[45], M. Pitt[175], L. Plazak[146a],
M.-A. Pleier[27], V. Pleskot[86], E. Plotnikova[68], D. Pluth[67], P. Podberezko[111], R. Poettgen[148a,148b],
L. Poggioli[119], D. Pohl[23], G. Polesello[123a], A. Poley[45], A. Policicchio[40a,40b], R. Polifka[32],
A. Polini[22a], C.S. Pollard[56], V. Polychronakos[27], K. Pommès[32], L. Pontecorvo[134a], B.G. Pope[93],
G.A. Popeneciu[28d], A. Poppleton[32], S. Pospisil[130], K. Potamianos[16], I.N. Potrap[68], C.J. Potter[30],
C.T. Potter[118], G. Poulard[32], J. Poveda[32], M.E. Pozo Astigarraga[32], P. Pralavorio[88], A. Pranko[16],
S. Prell[67], D. Price[87], L.E. Price[6], M. Primavera[76a], S. Prince[90], K. Prokofiev[62c], F. Prokoshin[34b],
S. Protopopescu[27], J. Proudfoot[6], M. Przybycien[41a], A. Puddu[136a,136b], A. Puri[169], P. Puzo[119],
J. Qian[92], G. Qin[56], Y. Qin[87], A. Quadt[57], W.B. Quayle[167a,167b], M. Queitsch-Maitland[45],
D. Quilty[56], S. Raddum[121], V. Radeka[27], V. Radescu[122], S.K. Radhakrishnan[150], P. Radloff[118],
P. Rados[91], F. Ragusa[94a,94b], G. Rahal[181], J.A. Raine[87], S. Rajagopalan[27], C. Rangel-Smith[168],
M.G. Ratti[94a,94b], D.M. Rauch[45], F. Rauscher[102], S. Rave[86], T. Ravenscroft[56], I. Ravinovich[175],
M. Raymond[32], A.L. Read[121], N.P. Readioff[77], M. Reale[76a,76b], D.M. Rebuzzi[123a,123b],
A. Redelbach[177], G. Redlinger[27], R. Reece[139], R.G. Reed[147c], K. Reeves[44], L. Rehnisch[17],
J. Reichert[124], A. Reiss[86], C. Rembser[32], H. Ren[35a], M. Rescigno[134a], S. Resconi[94a],
E.D. Resseguie[124], S. Rettie[171], E. Reynolds[19], O.L. Rezanova[111,c], P. Reznicek[131], R. Rezvani[97],
R. Richter[103], S. Richter[81], E. Richter-Was[41b], O. Ricken[23], M. Ridel[83], P. Rieck[103],
C.J. Riegel[178], J. Rieger[57], O. Rifki[115], M. Rijssenbeek[150], A. Rimoldi[123a,123b], M. Rimoldi[18],
L. Rinaldi[22a], B. Ristić[52], E. Ritsch[32], I. Riu[13], F. Rizatdinova[116], E. Rizvi[79], C. Rizzi[13],
R.T. Roberts[87], S.H. Robertson[90,n], A. Robichaud-Veronneau[90], D. Robinson[30],
J.E.M. Robinson[45], A. Robson[56], C. Roda[126a,126b], Y. Rodina[88,ak], A. Rodriguez Perez[13],
D. Rodriguez Rodriguez[170], S. Roe[32], C.S. Rogan[59], O. Røhne[121], J. Roloff[59], A. Romaniouk[100],
M. Romano[22a,22b], S.M. Romano Saez[37], E. Romero Adam[170], N. Rompotis[77], M. Ronzani[51],
L. Roos[83], S. Rosati[134a], K. Rosbach[51], P. Rose[139], N.-A. Rosien[57], V. Rossetti[148a,148b],
E. Rossi[106a,106b], L.P. Rossi[53a], J.H.N. Rosten[30], R. Rosten[140], M. Rotaru[28b], I. Roth[175],
J. Rothberg[140], D. Rousseau[119], A. Rozanov[88], Y. Rozen[154], X. Ruan[147c], F. Rubbo[145],
F. Rühr[51], A. Ruiz-Martinez[31], Z. Rurikova[51], N.A. Rusakovich[68], A. Ruschke[102], H.L. Russell[140],
J.P. Rutherfoord[7], N. Ruthmann[32], Y.F. Ryabov[125], M. Rybar[169], G. Rybkin[119], S. Ryu[6],
A. Ryzhov[132], G.F. Rzehorz[57], A.F. Saavedra[152], G. Sabato[109], S. Sacerdoti[29],
H.F-W. Sadrozinski[139], R. Sadykov[68], F. Safai Tehrani[134a], P. Saha[110], M. Sahinsoy[60a],
M. Saimpert[45], T. Saito[157], H. Sakamoto[157], Y. Sakurai[174], G. Salamanna[136a,136b],
J.E. Salazar Loyola[34b], D. Salek[109], P.H. Sales De Bruin[140], D. Salihagic[103], A. Salnikov[145],
J. Salt[170], D. Salvatore[40a,40b], F. Salvatore[151], A. Salvucci[62a,62b,62c], A. Salzburger[32],
D. Sammel[51], D. Sampsonidis[156], J. Sánchez[170], V. Sanchez Martinez[170],
A. Sanchez Pineda[106a,106b], H. Sandaker[121], R.L. Sandbach[79], C.O. Sander[45], M. Sandhoff[178],
C. Sandoval[21], D.P.C. Sankey[133], M. Sannino[53a,53b], A. Sansoni[50], C. Santoni[37],
R. Santonico[135a,135b], H. Santos[128a], I. Santoyo Castillo[151], K. Sapp[127], A. Sapronov[68],
J.G. Saraiva[128a,128d], B. Sarrazin[23], O. Sasaki[69], K. Sato[164], E. Sauvan[5], G. Savage[80],
P. Savard[161,d], N. Savic[103], C. Sawyer[133], L. Sawyer[82,s], J. Saxon[33], C. Sbarra[22a],

A. Sbrizzi[22a,22b], T. Scanlon[81], D.A. Scannicchio[166], M. Scarcella[152], V. Scarfone[40a,40b],
J. Schaarschmidt[140], P. Schacht[103], B.M. Schachtner[102], D. Schaefer[32], L. Schaefer[124],
R. Schaefer[45], J. Schaeffer[86], S. Schaepe[23], S. Schaetzel[60b], U. Schäfer[86], A.C. Schaffer[119],
D. Schaile[102], R.D. Schamberger[150], V. Scharf[60a], V.A. Schegelsky[125], D. Scheirich[131],
M. Schernau[166], C. Schiavi[53a,53b], S. Schier[139], C. Schillo[51], M. Schioppa[40a,40b], S. Schlenker[32],
K.R. Schmidt-Sommerfeld[103], K. Schmieden[32], C. Schmitt[86], S. Schmitt[45], S. Schmitz[86],
B. Schneider[163a], U. Schnoor[51], L. Schoeffel[138], A. Schoening[60b], B.D. Schoenrock[93], E. Schopf[23],
M. Schott[86], J.F.P. Schouwenberg[108], J. Schovancova[8], S. Schramm[52], N. Schuh[86], A. Schulte[86],
M.J. Schultens[23], H.-C. Schultz-Coulon[60a], H. Schulz[17], M. Schumacher[51], B.A. Schumm[139],
Ph. Schune[138], A. Schwartzman[145], T.A. Schwarz[92], H. Schweiger[87], Ph. Schwemling[138],
R. Schwienhorst[93], J. Schwindling[138], T. Schwindt[23], G. Sciolla[25], F. Scuri[126a,126b], F. Scutti[91],
J. Searcy[92], P. Seema[23], S.C. Seidel[107], A. Seiden[139], J.M. Seixas[26a], G. Sekhniaidze[106a],
K. Sekhon[92], S.J. Sekula[43], N. Semprini-Cesari[22a,22b], C. Serfon[121], L. Serin[119], L. Serkin[167a,167b],
M. Sessa[136a,136b], R. Seuster[172], H. Severini[115], T. Sfiligoj[78], F. Sforza[32], A. Sfyrla[52],
E. Shabalina[57], N.W. Shaikh[148a,148b], L.Y. Shan[35a], R. Shang[169], J.T. Shank[24], M. Shapiro[16],
P.B. Shatalov[99], K. Shaw[167a,167b], S.M. Shaw[87], A. Shcherbakova[148a,148b], C.Y. Shehu[151],
Y. Shen[115], P. Sherwood[81], L. Shi[153,al], S. Shimizu[70], C.O. Shimmin[166], M. Shimojima[104],
S. Shirabe[73], M. Shiyakova[68,am], J. Shlomi[175], A. Shmeleva[98], D. Shoaleh Saadi[97],
M.J. Shochet[33], S. Shojaii[94a], D.R. Shope[115], S. Shrestha[113], E. Shulga[100], M.A. Shupe[7],
P. Sicho[129], A.M. Sickles[169], P.E. Sidebo[149], E. Sideras Haddad[147c], O. Sidiropoulou[177],
D. Sidorov[116], A. Sidoti[22a,22b], F. Siegert[47], Dj. Sijacki[14], J. Silva[128a,128d], S.B. Silverstein[148a],
V. Simak[130], Lj. Simic[14], S. Simion[119], E. Simioni[86], B. Simmons[81], M. Simon[86], P. Sinervo[161],
N.B. Sinev[118], M. Sioli[22a,22b], G. Siragusa[177], I. Siral[92], S.Yu. Sivoklokov[101], J. Sjölin[148a,148b],
M.B. Skinner[75], P. Skubic[115], M. Slater[19], T. Slavicek[130], M. Slawinska[109], K. Sliwa[165],
R. Slovak[131], V. Smakhtin[175], B.H. Smart[5], L. Smestad[15], J. Smiesko[146a], S.Yu. Smirnov[100],
Y. Smirnov[100], L.N. Smirnova[101,an], O. Smirnova[84], J.W. Smith[57], M.N.K. Smith[38],
R.W. Smith[38], M. Smizanska[75], K. Smolek[130], A.A. Snesarev[98], I.M. Snyder[118], S. Snyder[27],
R. Sobie[172,n], F. Socher[47], A. Soffer[155], D.A. Soh[153], G. Sokhrannyi[78], C.A. Solans Sanchez[32],
M. Solar[130], E.Yu. Soldatov[100], U. Soldevila[170], A.A. Solodkov[132], A. Soloshenko[68],
O.V. Solovyanov[132], V. Solovyev[125], P. Sommer[51], H. Son[165], H.Y. Song[36a,ao], A. Sopczak[130],
V. Sorin[13], D. Sosa[60b], C.L. Sotiropoulou[126a,126b], R. Soualah[167a,167c], A.M. Soukharev[111,c],
D. South[45], B.C. Sowden[80], S. Spagnolo[76a,76b], M. Spalla[126a,126b], M. Spangenberg[173],
F. Spanò[80], D. Sperlich[17], F. Spettel[103], T.M. Spieker[60a], R. Spighi[22a], G. Spigo[32], L.A. Spiller[91],
M. Spousta[131], R.D. St. Denis[56,*], A. Stabile[94a], R. Stamen[60a], S. Stamm[17], E. Stanecka[42],
R.W. Stanek[6], C. Stanescu[136a], M.M. Stanitzki[45], S. Stapnes[121], E.A. Starchenko[132],
G.H. Stark[33], J. Stark[58], S.H Stark[39], P. Staroba[129], P. Starovoitov[60a], S. Stärz[32],
R. Staszewski[42], P. Steinberg[27], B. Stelzer[144], H.J. Stelzer[32], O. Stelzer-Chilton[163a], H. Stenzel[55],
G.A. Stewart[56], J.A. Stillings[23], M.C. Stockton[90], M. Stoebe[90], G. Stoicea[28b], P. Stolte[57],
S. Stonjek[103], A.R. Stradling[8], A. Straessner[47], M.E. Stramaglia[18], J. Strandberg[149],
S. Strandberg[148a,148b], A. Strandlie[121], M. Strauss[115], P. Strizenec[146b], R. Ströhmer[177],
D.M. Strom[118], R. Stroynowski[43], A. Strubig[108], S.A. Stucci[27], B. Stugu[15], N.A. Styles[45],
D. Su[145], J. Su[127], S. Suchek[60a], Y. Sugaya[120], M. Suk[130], V.V. Sulin[98], S. Sultansoy[4c],
T. Sumida[71], S. Sun[59], X. Sun[3], K. Suruliz[151], C.J.E. Suster[152], M.R. Sutton[151], S. Suzuki[69],
M. Svatos[129], M. Swiatlowski[33], S.P. Swift[2], I. Sykora[146a], T. Sykora[131], D. Ta[51], K. Tackmann[45],
J. Taenzer[155], A. Taffard[166], R. Tafirout[163a], N. Taiblum[155], H. Takai[27], R. Takashima[72],
T. Takeshita[142], Y. Takubo[69], M. Talby[88], A.A. Talyshev[111,c], J. Tanaka[157], M. Tanaka[159],
R. Tanaka[119], S. Tanaka[69], R. Tanioka[70], B.B. Tannenwald[113], S. Tapia Araya[34b], S. Tapprogge[86],
S. Tarem[154], G.F. Tartarelli[94a], P. Tas[131], M. Tasevsky[129], T. Tashiro[71], E. Tassi[40a,40b],

A. Tavares Delgado[128a,128b], Y. Tayalati[137e], A.C. Taylor[107], G.N. Taylor[91], P.T.E. Taylor[91],
W. Taylor[163b], P. Teixeira-Dias[80], K.K. Temming[51], D. Temple[144], H. Ten Kate[32], P.K. Teng[153],
J.J. Teoh[120], F. Tepel[178], S. Terada[69], K. Terashi[157], J. Terron[85], S. Terzo[13], M. Testa[50],
R.J. Teuscher[161,n], T. Theveneaux-Pelzer[88], J.P. Thomas[19], J. Thomas-Wilsker[80],
P.D. Thompson[19], A.S. Thompson[56], L.A. Thomsen[179], E. Thomson[124], M.J. Tibbetts[16],
R.E. Ticse Torres[88], V.O. Tikhomirov[98,ap], Yu.A. Tikhonov[111,c], S. Timoshenko[100], P. Tipton[179],
S. Tisserant[88], K. Todome[159], S. Todorova-Nova[5], J. Tojo[73], S. Tokár[146a], K. Tokushuku[69],
E. Tolley[59], L. Tomlinson[87], M. Tomoto[105], L. Tompkins[145,aq], K. Toms[107], B. Tong[59],
P. Tornambe[51], E. Torrence[118], H. Torres[144], E. Torró Pastor[140], J. Toth[88,ar], F. Touchard[88],
D.R. Tovey[141], C.J. Treado[112], T. Trefzger[177], A. Tricoli[27], I.M. Trigger[163a], S. Trincaz-Duvoid[83],
M.F. Tripiana[13], W. Trischuk[161], B. Trocmé[58], A. Trofymov[45], C. Troncon[94a],
M. Trottier-McDonald[16], M. Trovatelli[172], L. Truong[167a,167c], M. Trzebinski[42], A. Trzupek[42],
K.W. Tsang[62a], J.C-L. Tseng[122], P.V. Tsiareshka[95], G. Tsipolitis[10], N. Tsirintanis[9],
S. Tsiskaridze[13], V. Tsiskaridze[51], E.G. Tskhadadze[54a], K.M. Tsui[62a], I.I. Tsukerman[99],
V. Tsulaia[16], S. Tsuno[69], D. Tsybychev[150], Y. Tu[62b], A. Tudorache[28b], V. Tudorache[28b],
T.T. Tulbure[28a], A.N. Tuna[59], S.A. Tupputi[22a,22b], S. Turchikhin[68], D. Turgeman[175],
I. Turk Cakir[4b,as], R. Turra[94a,94b], P.M. Tuts[38], G. Ucchielli[22a,22b], I. Ueda[69], M. Ughetto[148a,148b],
F. Ukegawa[164], G. Unal[32], A. Undrus[27], G. Unel[166], F.C. Ungaro[91], Y. Unno[69],
C. Unverdorben[102], J. Urban[146b], P. Urquijo[91], P. Urrejola[86], G. Usai[8], J. Usui[69], L. Vacavant[88],
V. Vacek[130], B. Vachon[90], C. Valderanis[102], E. Valdes Santurio[148a,148b], N. Valencic[109],
S. Valentinetti[22a,22b], A. Valero[170], L. Valery[13], S. Valkar[131], A. Vallier[5], J.A. Valls Ferrer[170],
W. Van Den Wollenberg[109], H. van der Graaf[109], N. van Eldik[154], P. van Gemmeren[6],
J. Van Nieuwkoop[144], I. van Vulpen[109], M.C. van Woerden[109], M. Vanadia[134a,134b],
W. Vandelli[32], R. Vanguri[124], A. Vaniachine[160], P. Vankov[109], G. Vardanyan[180], R. Vari[134a],
E.W. Varnes[7], C. Varni[53a,53b], T. Varol[43], D. Varouchas[83], A. Vartapetian[8], K.E. Varvell[152],
J.G. Vasquez[179], G.A. Vasquez[34b], F. Vazeille[37], T. Vazquez Schroeder[90], J. Veatch[57],
V. Veeraraghavan[7], L.M. Veloce[161], F. Veloso[128a,128c], S. Veneziano[134a], A. Ventura[76a,76b],
M. Venturi[172], N. Venturi[161], A. Venturini[25], V. Vercesi[123a], M. Verducci[136a,136b], W. Verkerke[109],
J.C. Vermeulen[109], M.C. Vetterli[144,d], N. Viaux Maira[34a], O. Viazlo[84], I. Vichou[169,*],
T. Vickey[141], O.E. Vickey Boeriu[141], G.H.A. Viehhauser[122], S. Viel[16], L. Vigani[122],
M. Villa[22a,22b], M. Villaplana Perez[94a,94b], E. Vilucchi[50], M.G. Vincter[31], V.B. Vinogradov[68],
A. Vishwakarma[45], C. Vittori[22a,22b], I. Vivarelli[151], S. Vlachos[10], M. Vlasak[130], M. Vogel[178],
P. Vokac[130], G. Volpi[126a,126b], M. Volpi[91], H. von der Schmitt[103], E. von Toerne[23], V. Vorobel[131],
K. Vorobev[100], M. Vos[170], R. Voss[32], J.H. Vossebeld[77], M. Vozak[129], N. Vranjes[14],
M. Vranjes Milosavljevic[14], V. Vrba[130], M. Vreeswijk[109], R. Vuillermet[32], I. Vukotic[33],
P. Wagner[23], W. Wagner[178], H. Wahlberg[74], S. Wahrmund[47], J. Wakabayashi[105], J. Walder[75],
R. Walker[102], W. Walkowiak[143], V. Wallangen[148a,148b], C. Wang[35b], C. Wang[36b,at], F. Wang[176],
H. Wang[16], H. Wang[3], J. Wang[45], J. Wang[152], Q. Wang[115], R. Wang[6], S.M. Wang[153], T. Wang[38],
W. Wang[153,au], W. Wang[36a], C. Wanotayaroj[118], A. Warburton[90], C.P. Ward[30],
D.R. Wardrope[81], A. Washbrook[49], P.M. Watkins[19], A.T. Watson[19], M.F. Watson[19], G. Watts[140],
S. Watts[87], B.M. Waugh[81], A.F. Webb[11], S. Webb[86], M.S. Weber[18], S.W. Weber[177],
S.A. Weber[31], J.S. Webster[6], A.R. Weidberg[122], B. Weinert[64], J. Weingarten[57], C. Weiser[51],
H. Weits[109], P.S. Wells[32], T. Wenaus[27], T. Wengler[32], S. Wenig[32], N. Wermes[23], M.D. Werner[67],
P. Werner[32], M. Wessels[60a], K. Whalen[118], N.L. Whallon[140], A.M. Wharton[75], A. White[8],
M.J. White[1], R. White[34b], D. Whiteson[166], F.J. Wickens[133], W. Wiedenmann[176], M. Wielers[133],
C. Wiglesworth[39], L.A.M. Wiik-Fuchs[23], A. Wildauer[103], F. Wilk[87], H.G. Wilkens[32],
H.H. Williams[124], S. Williams[109], C. Willis[93], S. Willocq[89], J.A. Wilson[19], I. Wingerter-Seez[5],
F. Winklmeier[118], O.J. Winston[151], B.T. Winter[23], M. Wittgen[145], M. Wobisch[82,s],

T.M.H. Wolf[109], R. Wolff[88], M.W. Wolter[42], H. Wolters[128a,128c], S.D. Worm[133], B.K. Wosiek[42], J. Wotschack[32], M.J. Woudstra[87], K.W. Wozniak[42], M. Wu[33], S.L. Wu[176], X. Wu[52], Y. Wu[92], T.R. Wyatt[87], B.M. Wynne[49], S. Xella[39], Z. Xi[92], L. Xia[35c], D. Xu[35a], L. Xu[27], B. Yabsley[152], S. Yacoob[147a], D. Yamaguchi[159], Y. Yamaguchi[120], A. Yamamoto[69], S. Yamamoto[157], T. Yamanaka[157], K. Yamauchi[105], Y. Yamazaki[70], Z. Yan[24], H. Yang[36c], H. Yang[16], Y. Yang[153], Z. Yang[15], W-M. Yao[16], Y.C. Yap[83], Y. Yasu[69], E. Yatsenko[5], K.H. Yau Wong[23], J. Ye[43], S. Ye[27], I. Yeletskikh[68], E. Yildirim[86], K. Yorita[174], K. Yoshihara[124], C. Young[145], C.J.S. Young[32], S. Youssef[24], D.R. Yu[16], J. Yu[8], J. Yu[67], L. Yuan[70], S.P.Y. Yuen[23], I. Yusuff[30,av], B. Zabinski[42], G. Zacharis[10], R. Zaidan[13], A.M. Zaitsev[132,ah], N. Zakharchuk[45], J. Zalieckas[15], A. Zaman[150], S. Zambito[59], D. Zanzi[91], C. Zeitnitz[178], M. Zeman[130], A. Zemla[41a], J.C. Zeng[169], Q. Zeng[145], O. Zenin[132], T. Ženiš[146a], D. Zerwas[119], D. Zhang[92], F. Zhang[176], G. Zhang[36a,ao], H. Zhang[35b], J. Zhang[6], L. Zhang[51], L. Zhang[36a], M. Zhang[169], R. Zhang[23], R. Zhang[36a,at], X. Zhang[36b], Y. Zhang[35a], Z. Zhang[119], X. Zhao[43], Y. Zhao[36b,aw], Z. Zhao[36a], A. Zhemchugov[68], J. Zhong[122], B. Zhou[92], C. Zhou[176], L. Zhou[43], M. Zhou[35a], M. Zhou[150], N. Zhou[35c], C.G. Zhu[36b], H. Zhu[35a], J. Zhu[92], Y. Zhu[36a], X. Zhuang[35a], K. Zhukov[98], A. Zibell[177], D. Zieminska[64], N.I. Zimine[68], C. Zimmermann[86], S. Zimmermann[51], Z. Zinonos[103], M. Zinser[86], M. Ziolkowski[143], L. Živković[14], G. Zobernig[176], A. Zoccoli[22a,22b], R. Zou[33], M. zur Nedden[17] and L. Zwalinski[32]

1 Department of Physics, University of Adelaide, Adelaide, Australia
2 Physics Department, SUNY Albany, Albany NY, United States of America
3 Department of Physics, University of Alberta, Edmonton AB, Canada
4 [a] Department of Physics, Ankara University, Ankara; [b] Istanbul Aydin University, Istanbul; [c] Division of Physics, TOBB University of Economics and Technology, Ankara, Turkey
5 LAPP, CNRS/IN2P3 and Université Savoie Mont Blanc, Annecy-le-Vieux, France
6 High Energy Physics Division, Argonne National Laboratory, Argonne IL, United States of America
7 Department of Physics, University of Arizona, Tucson AZ, United States of America
8 Department of Physics, The University of Texas at Arlington, Arlington TX, United States of America
9 Physics Department, National and Kapodistrian University of Athens, Athens, Greece
10 Physics Department, National Technical University of Athens, Zografou, Greece
11 Department of Physics, The University of Texas at Austin, Austin TX, United States of America
12 Institute of Physics, Azerbaijan Academy of Sciences, Baku, Azerbaijan
13 Institut de Física d'Altes Energies (IFAE), The Barcelona Institute of Science and Technology, Barcelona, Spain
14 Institute of Physics, University of Belgrade, Belgrade, Serbia
15 Department for Physics and Technology, University of Bergen, Bergen, Norway
16 Physics Division, Lawrence Berkeley National Laboratory and University of California, Berkeley CA, United States of America
17 Department of Physics, Humboldt University, Berlin, Germany
18 Albert Einstein Center for Fundamental Physics and Laboratory for High Energy Physics, University of Bern, Bern, Switzerland
19 School of Physics and Astronomy, University of Birmingham, Birmingham, United Kingdom
20 [a] Department of Physics, Bogazici University, Istanbul; [b] Department of Physics Engineering, Gaziantep University, Gaziantep; [d] Istanbul Bilgi University, Faculty of Engineering and Natural Sciences, Istanbul,Turkey; [e] Bahcesehir University, Faculty of Engineering and Natural Sciences, Istanbul, Turkey, Turkey
21 Centro de Investigaciones, Universidad Antonio Narino, Bogota, Colombia
22 [a] INFN Sezione di Bologna; [b] Dipartimento di Fisica e Astronomia, Università di Bologna, Bologna, Italy
23 Physikalisches Institut, University of Bonn, Bonn, Germany
24 Department of Physics, Boston University, Boston MA, United States of America

25 _Department of Physics, Brandeis University, Waltham MA, United States of America_

26 _(a) Universidade Federal do Rio De Janeiro COPPE/EE/IF, Rio de Janeiro; (b) Electrical Circuits Department, Federal University of Juiz de Fora (UFJF), Juiz de Fora; (c) Federal University of Sao Joao del Rei (UFSJ), Sao Joao del Rei; (d) Instituto de Fisica, Universidade de Sao Paulo, Sao Paulo, Brazil_

27 _Physics Department, Brookhaven National Laboratory, Upton NY, United States of America_

28 _(a) Transilvania University of Brasov, Brasov, Romania; (b) Horia Hulubei National Institute of Physics and Nuclear Engineering, Bucharest; (c) Department of Physics, Alexandru Ioan Cuza University of Iasi, Iasi, Romania; (d) National Institute for Research and Development of Isotopic and Molecular Technologies, Physics Department, Cluj Napoca; (e) University Politehnica Bucharest, Bucharest; (f) West University in Timisoara, Timisoara, Romania_

29 _Departamento de Física, Universidad de Buenos Aires, Buenos Aires, Argentina_

30 _Cavendish Laboratory, University of Cambridge, Cambridge, United Kingdom_

31 _Department of Physics, Carleton University, Ottawa ON, Canada_

32 _CERN, Geneva, Switzerland_

33 _Enrico Fermi Institute, University of Chicago, Chicago IL, United States of America_

34 _(a) Departamento de Física, Pontificia Universidad Católica de Chile, Santiago; (b) Departamento de Física, Universidad Técnica Federico Santa María, Valparaíso, Chile_

35 _(a) Institute of High Energy Physics, Chinese Academy of Sciences, Beijing; (b) Department of Physics, Nanjing University, Jiangsu; (c) Physics Department, Tsinghua University, Beijing 100084, China_

36 _(a) Department of Modern Physics, University of Science and Technology of China, Anhui; (b) School of Physics, Shandong University, Shandong; (c) Department of Physics and Astronomy, Key Laboratory for Particle Physics, Astrophysics and Cosmology, Ministry of Education; Shanghai Key Laboratory for Particle Physics and Cosmology (SKLPPC), Shanghai Jiao Tong University, Shanghai;, China_

37 _Laboratoire de Physique Corpusculaire, Université Clermont Auvergne, Université Blaise Pascal, CNRS/IN2P3, Clermont-Ferrand, France_

38 _Nevis Laboratory, Columbia University, Irvington NY, United States of America_

39 _Niels Bohr Institute, University of Copenhagen, Kobenhavn, Denmark_

40 _(a) INFN Gruppo Collegato di Cosenza, Laboratori Nazionali di Frascati; (b) Dipartimento di Fisica, Università della Calabria, Rende, Italy_

41 _(a) AGH University of Science and Technology, Faculty of Physics and Applied Computer Science, Krakow; (b) Marian Smoluchowski Institute of Physics, Jagiellonian University, Krakow, Poland_

42 _Institute of Nuclear Physics Polish Academy of Sciences, Krakow, Poland_

43 _Physics Department, Southern Methodist University, Dallas TX, United States of America_

44 _Physics Department, University of Texas at Dallas, Richardson TX, United States of America_

45 _DESY, Hamburg and Zeuthen, Germany_

46 _Lehrstuhl für Experimentelle Physik IV, Technische Universität Dortmund, Dortmund, Germany_

47 _Institut für Kern- und Teilchenphysik, Technische Universität Dresden, Dresden, Germany_

48 _Department of Physics, Duke University, Durham NC, United States of America_

49 _SUPA - School of Physics and Astronomy, University of Edinburgh, Edinburgh, United Kingdom_

50 _INFN Laboratori Nazionali di Frascati, Frascati, Italy_

51 _Fakultät für Mathematik und Physik, Albert-Ludwigs-Universität, Freiburg, Germany_

52 _Departement de Physique Nucleaire et Corpusculaire, Université de Genève, Geneva, Switzerland_

53 _(a) INFN Sezione di Genova; (b) Dipartimento di Fisica, Università di Genova, Genova, Italy_

54 _(a) E. Andronikashvili Institute of Physics, Iv. Javakhishvili Tbilisi State University, Tbilisi; (b) High Energy Physics Institute, Tbilisi State University, Tbilisi, Georgia_

55 _II Physikalisches Institut, Justus-Liebig-Universität Giessen, Giessen, Germany_

56 _SUPA - School of Physics and Astronomy, University of Glasgow, Glasgow, United Kingdom_

57 _II Physikalisches Institut, Georg-August-Universität, Göttingen, Germany_

58 _Laboratoire de Physique Subatomique et de Cosmologie, Université Grenoble-Alpes, CNRS/IN2P3, Grenoble, France_

[59] *Laboratory for Particle Physics and Cosmology, Harvard University, Cambridge MA, United States of America*

[60] *[a] Kirchhoff-Institut für Physik, Ruprecht-Karls-Universität Heidelberg, Heidelberg; [b] Physikalisches Institut, Ruprecht-Karls-Universität Heidelberg, Heidelberg; [c] ZITI Institut für technische Informatik, Ruprecht-Karls-Universität Heidelberg, Mannheim, Germany*

[61] *Faculty of Applied Information Science, Hiroshima Institute of Technology, Hiroshima, Japan*

[62] *[a] Department of Physics, The Chinese University of Hong Kong, Shatin, N.T., Hong Kong; [b] Department of Physics, The University of Hong Kong, Hong Kong; [c] Department of Physics and Institute for Advanced Study, The Hong Kong University of Science and Technology, Clear Water Bay, Kowloon, Hong Kong, China*

[63] *Department of Physics, National Tsing Hua University, Taiwan, Taiwan*

[64] *Department of Physics, Indiana University, Bloomington IN, United States of America*

[65] *Institut für Astro- und Teilchenphysik, Leopold-Franzens-Universität, Innsbruck, Austria*

[66] *University of Iowa, Iowa City IA, United States of America*

[67] *Department of Physics and Astronomy, Iowa State University, Ames IA, United States of America*

[68] *Joint Institute for Nuclear Research, JINR Dubna, Dubna, Russia*

[69] *KEK, High Energy Accelerator Research Organization, Tsukuba, Japan*

[70] *Graduate School of Science, Kobe University, Kobe, Japan*

[71] *Faculty of Science, Kyoto University, Kyoto, Japan*

[72] *Kyoto University of Education, Kyoto, Japan*

[73] *Department of Physics, Kyushu University, Fukuoka, Japan*

[74] *Instituto de Física La Plata, Universidad Nacional de La Plata and CONICET, La Plata, Argentina*

[75] *Physics Department, Lancaster University, Lancaster, United Kingdom*

[76] *[a] INFN Sezione di Lecce; [b] Dipartimento di Matematica e Fisica, Università del Salento, Lecce, Italy*

[77] *Oliver Lodge Laboratory, University of Liverpool, Liverpool, United Kingdom*

[78] *Department of Experimental Particle Physics, Jožef Stefan Institute and Department of Physics, University of Ljubljana, Ljubljana, Slovenia*

[79] *School of Physics and Astronomy, Queen Mary University of London, London, United Kingdom*

[80] *Department of Physics, Royal Holloway University of London, Surrey, United Kingdom*

[81] *Department of Physics and Astronomy, University College London, London, United Kingdom*

[82] *Louisiana Tech University, Ruston LA, United States of America*

[83] *Laboratoire de Physique Nucléaire et de Hautes Energies, UPMC and Université Paris-Diderot and CNRS/IN2P3, Paris, France*

[84] *Fysiska institutionen, Lunds universitet, Lund, Sweden*

[85] *Departamento de Fisica Teorica C-15, Universidad Autonoma de Madrid, Madrid, Spain*

[86] *Institut für Physik, Universität Mainz, Mainz, Germany*

[87] *School of Physics and Astronomy, University of Manchester, Manchester, United Kingdom*

[88] *CPPM, Aix-Marseille Université and CNRS/IN2P3, Marseille, France*

[89] *Department of Physics, University of Massachusetts, Amherst MA, United States of America*

[90] *Department of Physics, McGill University, Montreal QC, Canada*

[91] *School of Physics, University of Melbourne, Victoria, Australia*

[92] *Department of Physics, The University of Michigan, Ann Arbor MI, United States of America*

[93] *Department of Physics and Astronomy, Michigan State University, East Lansing MI, United States of America*

[94] *[a] INFN Sezione di Milano; [b] Dipartimento di Fisica, Università di Milano, Milano, Italy*

[95] *B.I. Stepanov Institute of Physics, National Academy of Sciences of Belarus, Minsk, Republic of Belarus*

[96] *Research Institute for Nuclear Problems of Byelorussian State University, Minsk, Republic of Belarus*

[97] *Group of Particle Physics, University of Montreal, Montreal QC, Canada*

[98] *P.N. Lebedev Physical Institute of the Russian Academy of Sciences, Moscow, Russia*

99 *Institute for Theoretical and Experimental Physics (ITEP), Moscow, Russia*
100 *National Research Nuclear University MEPhI, Moscow, Russia*
101 *D.V. Skobeltsyn Institute of Nuclear Physics, M.V. Lomonosov Moscow State University, Moscow, Russia*
102 *Fakultät für Physik, Ludwig-Maximilians-Universität München, München, Germany*
103 *Max-Planck-Institut für Physik (Werner-Heisenberg-Institut), München, Germany*
104 *Nagasaki Institute of Applied Science, Nagasaki, Japan*
105 *Graduate School of Science and Kobayashi-Maskawa Institute, Nagoya University, Nagoya, Japan*
106 *(a) INFN Sezione di Napoli; (b) Dipartimento di Fisica, Università di Napoli, Napoli, Italy*
107 *Department of Physics and Astronomy, University of New Mexico, Albuquerque NM, United States of America*
108 *Institute for Mathematics, Astrophysics and Particle Physics, Radboud University Nijmegen/Nikhef, Nijmegen, Netherlands*
109 *Nikhef National Institute for Subatomic Physics and University of Amsterdam, Amsterdam, Netherlands*
110 *Department of Physics, Northern Illinois University, DeKalb IL, United States of America*
111 *Budker Institute of Nuclear Physics, SB RAS, Novosibirsk, Russia*
112 *Department of Physics, New York University, New York NY, United States of America*
113 *Ohio State University, Columbus OH, United States of America*
114 *Faculty of Science, Okayama University, Okayama, Japan*
115 *Homer L. Dodge Department of Physics and Astronomy, University of Oklahoma, Norman OK, United States of America*
116 *Department of Physics, Oklahoma State University, Stillwater OK, United States of America*
117 *Palacký University, RCPTM, Olomouc, Czech Republic*
118 *Center for High Energy Physics, University of Oregon, Eugene OR, United States of America*
119 *LAL, Univ. Paris-Sud, CNRS/IN2P3, Université Paris-Saclay, Orsay, France*
120 *Graduate School of Science, Osaka University, Osaka, Japan*
121 *Department of Physics, University of Oslo, Oslo, Norway*
122 *Department of Physics, Oxford University, Oxford, United Kingdom*
123 *(a) INFN Sezione di Pavia; (b) Dipartimento di Fisica, Università di Pavia, Pavia, Italy*
124 *Department of Physics, University of Pennsylvania, Philadelphia PA, United States of America*
125 *National Research Centre "Kurchatov Institute" B.P.Konstantinov Petersburg Nuclear Physics Institute, St. Petersburg, Russia*
126 *(a) INFN Sezione di Pisa; (b) Dipartimento di Fisica E. Fermi, Università di Pisa, Pisa, Italy*
127 *Department of Physics and Astronomy, University of Pittsburgh, Pittsburgh PA, United States of America*
128 *(a) Laboratório de Instrumentação e Física Experimental de Partículas - LIP, Lisboa; (b) Faculdade de Ciências, Universidade de Lisboa, Lisboa; (c) Department of Physics, University of Coimbra, Coimbra; (d) Centro de Física Nuclear da Universidade de Lisboa, Lisboa; (e) Departamento de Fisica, Universidade do Minho, Braga; (f) Departamento de Fisica Teorica y del Cosmos and CAFPE, Universidad de Granada, Granada (Spain); (g) Dep Fisica and CEFITEC of Faculdade de Ciencias e Tecnologia, Universidade Nova de Lisboa, Caparica, Portugal*
129 *Institute of Physics, Academy of Sciences of the Czech Republic, Praha, Czech Republic*
130 *Czech Technical University in Prague, Praha, Czech Republic*
131 *Charles University, Faculty of Mathematics and Physics, Prague, Czech Republic*
132 *State Research Center Institute for High Energy Physics (Protvino), NRC KI, Russia*
133 *Particle Physics Department, Rutherford Appleton Laboratory, Didcot, United Kingdom*
134 *(a) INFN Sezione di Roma; (b) Dipartimento di Fisica, Sapienza Università di Roma, Roma, Italy*
135 *(a) INFN Sezione di Roma Tor Vergata; (b) Dipartimento di Fisica, Università di Roma Tor Vergata, Roma, Italy*
136 *(a) INFN Sezione di Roma Tre; (b) Dipartimento di Matematica e Fisica, Università Roma Tre, Roma, Italy*

137 (a) Faculté des Sciences Ain Chock, Réseau Universitaire de Physique des Hautes Energies - Université Hassan II, Casablanca; (b) Centre National de l'Energie des Sciences Techniques Nucleaires, Rabat; (c) Faculté des Sciences Semlalia, Université Cadi Ayyad, LPHEA-Marrakech; (d) Faculté des Sciences, Université Mohamed Premier and LPTPM, Oujda; (e) Faculté des sciences, Université Mohammed V, Rabat, Morocco

138 DSM/IRFU (Institut de Recherches sur les Lois Fondamentales de l'Univers), CEA Saclay (Commissariat à l'Energie Atomique et aux Energies Alternatives), Gif-sur-Yvette, France

139 Santa Cruz Institute for Particle Physics, University of California Santa Cruz, Santa Cruz CA, United States of America

140 Department of Physics, University of Washington, Seattle WA, United States of America

141 Department of Physics and Astronomy, University of Sheffield, Sheffield, United Kingdom

142 Department of Physics, Shinshu University, Nagano, Japan

143 Fachbereich Physik, Universität Siegen, Siegen, Germany

144 Department of Physics, Simon Fraser University, Burnaby BC, Canada

145 SLAC National Accelerator Laboratory, Stanford CA, United States of America

146 (a) Faculty of Mathematics, Physics & Informatics, Comenius University, Bratislava; (b) Department of Subnuclear Physics, Institute of Experimental Physics of the Slovak Academy of Sciences, Kosice, Slovak Republic

147 (a) Department of Physics, University of Cape Town, Cape Town; (b) Department of Physics, University of Johannesburg, Johannesburg; (c) School of Physics, University of the Witwatersrand, Johannesburg, South Africa

148 (a) Department of Physics, Stockholm University; (b) The Oskar Klein Centre, Stockholm, Sweden

149 Physics Department, Royal Institute of Technology, Stockholm, Sweden

150 Departments of Physics & Astronomy and Chemistry, Stony Brook University, Stony Brook NY, United States of America

151 Department of Physics and Astronomy, University of Sussex, Brighton, United Kingdom

152 School of Physics, University of Sydney, Sydney, Australia

153 Institute of Physics, Academia Sinica, Taipei, Taiwan

154 Department of Physics, Technion: Israel Institute of Technology, Haifa, Israel

155 Raymond and Beverly Sackler School of Physics and Astronomy, Tel Aviv University, Tel Aviv, Israel

156 Department of Physics, Aristotle University of Thessaloniki, Thessaloniki, Greece

157 International Center for Elementary Particle Physics and Department of Physics, The University of Tokyo, Tokyo, Japan

158 Graduate School of Science and Technology, Tokyo Metropolitan University, Tokyo, Japan

159 Department of Physics, Tokyo Institute of Technology, Tokyo, Japan

160 Tomsk State University, Tomsk, Russia, Russia

161 Department of Physics, University of Toronto, Toronto ON, Canada

162 (a) INFN-TIFPA; (b) University of Trento, Trento, Italy, Italy

163 (a) TRIUMF, Vancouver BC; (b) Department of Physics and Astronomy, York University, Toronto ON, Canada

164 Faculty of Pure and Applied Sciences, and Center for Integrated Research in Fundamental Science and Engineering, University of Tsukuba, Tsukuba, Japan

165 Department of Physics and Astronomy, Tufts University, Medford MA, United States of America

166 Department of Physics and Astronomy, University of California Irvine, Irvine CA, United States of America

167 (a) INFN Gruppo Collegato di Udine, Sezione di Trieste, Udine; (b) ICTP, Trieste; (c) Dipartimento di Chimica, Fisica e Ambiente, Università di Udine, Udine, Italy

168 Department of Physics and Astronomy, University of Uppsala, Uppsala, Sweden

169 Department of Physics, University of Illinois, Urbana IL, United States of America

170 Instituto de Fisica Corpuscular (IFIC) and Departamento de Fisica Atomica, Molecular y Nuclear and Departamento de Ingeniería Electrónica and Instituto de Microelectrónica de Barcelona (IMB-CNM), University of Valencia and CSIC, Valencia, Spain

[171] Department of Physics, University of British Columbia, Vancouver BC, Canada

[172] Department of Physics and Astronomy, University of Victoria, Victoria BC, Canada

[173] Department of Physics, University of Warwick, Coventry, United Kingdom

[174] Waseda University, Tokyo, Japan

[175] Department of Particle Physics, The Weizmann Institute of Science, Rehovot, Israel

[176] Department of Physics, University of Wisconsin, Madison WI, United States of America

[177] Fakultät für Physik und Astronomie, Julius-Maximilians-Universität, Würzburg, Germany

[178] Fakultät für Mathematik und Naturwissenschaften, Fachgruppe Physik, Bergische Universität Wuppertal, Wuppertal, Germany

[179] Department of Physics, Yale University, New Haven CT, United States of America

[180] Yerevan Physics Institute, Yerevan, Armenia

[181] Centre de Calcul de l'Institut National de Physique Nucléaire et de Physique des Particules (IN2P3), Villeurbanne, France

[a] Also at Department of Physics, King's College London, London, United Kingdom

[b] Also at Institute of Physics, Azerbaijan Academy of Sciences, Baku, Azerbaijan

[c] Also at Novosibirsk State University, Novosibirsk, Russia

[d] Also at TRIUMF, Vancouver BC, Canada

[e] Also at Department of Physics & Astronomy, University of Louisville, Louisville, KY, United States of America

[f] Also at Physics Department, An-Najah National University, Nablus, Palestine

[g] Also at Department of Physics, California State University, Fresno CA, United States of America

[h] Also at Department of Physics, University of Fribourg, Fribourg, Switzerland

[i] Also at Departament de Fisica de la Universitat Autonoma de Barcelona, Barcelona, Spain

[j] Also at Departamento de Fisica e Astronomia, Faculdade de Ciencias, Universidade do Porto, Portugal

[k] Also at Tomsk State University, Tomsk, Russia, Russia

[l] Also at The Collaborative Innovation Center of Quantum Matter (CICQM), Beijing, China

[m] Also at Universita di Napoli Parthenope, Napoli, Italy

[n] Also at Institute of Particle Physics (IPP), Canada

[o] Also at Horia Hulubei National Institute of Physics and Nuclear Engineering, Bucharest, Romania

[p] Also at Department of Physics, St. Petersburg State Polytechnical University, St. Petersburg, Russia

[q] Also at Department of Physics, The University of Michigan, Ann Arbor MI, United States of America

[r] Also at Centre for High Performance Computing, CSIR Campus, Rosebank, Cape Town, South Africa

[s] Also at Louisiana Tech University, Ruston LA, United States of America

[t] Also at Institucio Catalana de Recerca i Estudis Avancats, ICREA, Barcelona, Spain

[u] Also at Graduate School of Science, Osaka University, Osaka, Japan

[v] Also at Fakultät für Mathematik und Physik, Albert-Ludwigs-Universität, Freiburg, Germany

[w] Also at Institute for Mathematics, Astrophysics and Particle Physics, Radboud University Nijmegen/Nikhef, Nijmegen, Netherlands

[x] Also at Department of Physics, The University of Texas at Austin, Austin TX, United States of America

[y] Also at Institute of Theoretical Physics, Ilia State University, Tbilisi, Georgia

[z] Also at CERN, Geneva, Switzerland

[aa] Also at Georgian Technical University (GTU),Tbilisi, Georgia

[ab] Also at Ochadai Academic Production, Ochanomizu University, Tokyo, Japan

[ac] Also at Manhattan College, New York NY, United States of America

[ad] Also at Academia Sinica Grid Computing, Institute of Physics, Academia Sinica, Taipei, Taiwan

[ae] Also at School of Physics, Shandong University, Shandong, China

^{af} Also at Departamento de Fisica Teorica y del Cosmos and CAFPE, Universidad de Granada, Granada (Spain), Portugal

^{ag} Also at Department of Physics, California State University, Sacramento CA, United States of America

^{ah} Also at Moscow Institute of Physics and Technology State University, Dolgoprudny, Russia

^{ai} Also at Departement de Physique Nucleaire et Corpusculaire, Université de Genève, Geneva, Switzerland

^{aj} Also at International School for Advanced Studies (SISSA), Trieste, Italy

^{ak} Also at Institut de Física d'Altes Energies (IFAE), The Barcelona Institute of Science and Technology, Barcelona, Spain

^{al} Also at School of Physics, Sun Yat-sen University, Guangzhou, China

^{am} Also at Institute for Nuclear Research and Nuclear Energy (INRNE) of the Bulgarian Academy of Sciences, Sofia, Bulgaria

^{an} Also at Faculty of Physics, M.V.Lomonosov Moscow State University, Moscow, Russia

^{ao} Also at Institute of Physics, Academia Sinica, Taipei, Taiwan

^{ap} Also at National Research Nuclear University MEPhI, Moscow, Russia

^{aq} Also at Department of Physics, Stanford University, Stanford CA, United States of America

^{ar} Also at Institute for Particle and Nuclear Physics, Wigner Research Centre for Physics, Budapest, Hungary

^{as} Also at Giresun University, Faculty of Engineering, Turkey

^{at} Also at CPPM, Aix-Marseille Université and CNRS/IN2P3, Marseille, France

^{au} Also at Department of Physics, Nanjing University, Jiangsu, China

^{av} Also at University of Malaya, Department of Physics, Kuala Lumpur, Malaysia

^{aw} Also at LAL, Univ. Paris-Sud, CNRS/IN2P3, Université Paris-Saclay, Orsay, France

* Deceased